VERIFICATION OF MODELED PHOTON BEAM ATTENUATION OF TREATMENT COUCH TOP IN ONCENTRA MASTERPLAN TREATMENT PLANNING SYSTEM

This thesis / dissertation is submitted to the University of Ghana, Legon in partial fulfilment of the requirement for the award of **MPHIL Medical Physics degree**.

BY

BELINDA BUERMLE ASAMANYUAH

(10551189)

JULY, 2017

DECLARATION

This thesis is the result of research work carried out by Belinda Buermle Asamanyuah in the Department of Medical Physics, School of Nuclear and Allied Sciences, University of Ghana, under the supervision of Prof. Augustine W. K. Kyere, Dr. Francis Hasford and Mr. George Felix Acquah.

I hereby affirm that, no part of this work has been presented in part or whole to any other university or institution for the award of a diploma, or degree at any level. Accordingly other works and/or researches done by other researchers cited in this work have been acknowledged under references.

Sign …………………………
Belinda Buermle Asamanyuah
(Student)

Date………………………

Sign…………………………
Dr. Francis Hasford
(Principal Supervisor)

Date………………………

Sign…………………………
Prof. Augustine W. K. Kyere
(Co-Supervisor)
Date………………………

Sign…………………………
Mr. George Felix Acquah
(Co-Supervisor)
Date……………………

DEDICATION

I dedicate this work to my parents, Mr Edward Adinortey Asamanyuah and Mrs Felicia Maku Asamanyuah and my siblings.

ACKNOWLEDGEMENTS

With a grateful heart, I want to specially thank my supervisors Dr. Francis Hasford, Prof. Augustine W. K. Kyere and Mr. George Felix Acquah for fastidiously going through my write up and guiding me through my data collection, not forgetting their constructive criticisms, corrections, encouragement and wise counsels throughout the period of putting together this thesis.

Sincere thanks to the staff of Sweden Ghana Medical Centre, especially Mr. Philip O. Kyeremeh and the other staffs of the oncology department for their immense help in making available the resources to come up with this beautiful work and not forgetting Mr. Nicholas Liassidji of the cafeteria for boosting my vitality with his sumptuous meal.

To the ever young grandpa, Dr. Thomas T. Akiti, your indefectus love and cordatus counsels and the never insulus environment are the special features that have contributed to the balance in the psychological state I needed to be in, for a successful completion of this research. Thanks for using your rich international scientific experience in grooming my infant science life. I will always be grateful.

To my cherished friends, Mark Pokoo-Aikins (GAEC), Johnson Abusah Lorlornyo (SNAS), Daniel Ackom, Castrol Dumenya (SNAS), Philip Nii Amon Kotey (University of Ghana), Azu Akutey (KBTH-NCNMR), Ebenezer Osei, Prince Abban and Ernest Adusah. It has been your constant encouragement and love that I have relied upon throughout my time at the University. To the fine dominus and adcuratio Mr. Baffour Asare Mensah, I am truly grateful for your love and support throughout my study period.

Lastly, and most importantly, I wish to extend my heartfelt appreciation to my dear parents and my siblings; Mr. Richard Buertey Asamanyuah, Richard Tei, Mrs. Audery Buerkie Danso, Rosemary Buerkwor Asamanyuah and Emelia Maku Asamanyuah for their prayers and monetary support throughout my academic ladder.

Indeed, I will worship my maker, I will exalt his name for his goodness and mercies endureth forever. I will praise him! I will praise him! I will praise the LORD.

TABLE OF CONTENT

LIST OF FIGURES

LIST OF TABLES

APPENDICES

ABBREVIATIONS

2D	Two Dimensional
3D	Three Dimensional
ACF	Attenuation Correction Factor
AF	Attenuation Factor
ART	Alderson Radiation Therapy
BEV	Beam's Eye View
CFC	Carbon Fiber Couch
CRT	Conformal Radiotherapy
CT	Computed Tomography
DNA	Deoxyribonucleic Acid
EBRT	External Beam Radiotherapy
HU	Hounsfield Units
IAEA	International Atomic Energy Agency
ICRP	International Commission on Radiological Protection
ICRU	International Commission on Radiation Units and Measurements
IGRT	Image Guided Radiotherapy
IMRT	Intensity Modulated Radiotherapy
KBTH	Korle-Bu Teaching Hospital

LINAC	Linear Accelerator
MRI	Magnetic Resonance Imaging
MU	Monitor Units
MV	Megavolts
NCRNM	National Centre for Radiotherapy and Nuclear Medicine
PET	Positron Emission Tomography
PMMA	Polymethylmethacrylate
SABR	Stereotactic Ablative Body Radiotherapy
TBI	Total Body Irradiation
TPS	Treatment Planning System
VMAT	Volumetric Modulated Arc Therapy
WET	Water Equivalent Thickness
PTV	Planning Tumour Volume
MLC	Multileaf Collimator
SAD	Source to Axis Distance
SGMC	Sweden Ghana Medical Center
SSD	Source to Surface Distance
TF	Transmission Factor

ABSTRACT

During radiotherapy, some accessories used gets into the path of the photon beams. These somehow attenuate the beam to some extent. Therefore it is imperative that every radiotherapy facility quantifies the degree by which these accessories attenuate the beams. This informs the facility operators on the necessary corrections to make to achieve the desired dose to the target area. The purpose of this study was to evaluate the attenuation effects of 6 MV and 15 MV photon beam by an iBeam evo carbon fiber couch top and subsequently correct these effects by using the correction factor method. The couch was first CT scanned to verify it homogeneous construction. Ion chamber output measurements were carried out using polymethylmethacrylate PPMA, phantom. At normal incidence of both photon beams, the 6 MV beam was attenuated by 3.8%, 4.91%, 2.71% and 2.43% and the 15 MV beam by 2.43%, 3.86%, 1.57% and 1.35% at 5, 10, 15 and 20 cm^2 field size respectively. An equation for attenuation correction was worked out and correction factors for gantry angles 90° to 180° were obtained. Finally, these correction factors were applied in a typical pelvic case using an anthropomorphic phantom and an AB mimator diode. Photon beam attenuation by iBeam evo couch was well corrected by the correction factors when TPS calculated doses were compared to diode measurements. In conclusion, photon beam attenuation by a carbon fiber couch top was dependent on the gantry angle, field size and photon beam energy. This method using the correction factors was useful in correcting the isocenter dose when attenuation effects cannot be corrected by a treatment planning system. Clinical validation was done with an anthropomorphic phantom and AB Mimator diode dosimetry.

CHAPTER ONE

INTRODUCTION

1.1 BACKGROUND

In radiotherapy, the primary aim is to deliver an optimal dose to the target volume whilst minimizing dose to the surrounding normal tissues. This aim is usually achieved in external beam radiation therapy by using several beams to obtain a uniform dose distribution inside the target volume and to reduce normal tissue complications. Orientation of these multiple beams is attained by using different gantry angles. External beam radiotherapy techniques require the use of positioning and immobilization devices for localization of tumour and reproducibility of treatment procedures and so patients who are due for radiotherapy are treated using these devices. Such devices include couch tops, head and neck rest, knee support, vacuum pillows, leg rest, head mask, breast board, immobilization cast fixation plate or any other supportive device that has a high tensile strength of low weight and less beam attenuation. Materials used in the manufacturing these devices have the ability to attenuate and scatter the radiation beam which transits through them hence the dosimetric impact from these devices external to the patient is a combination of lesser skin sparing, reduced tumour dose and a modified dose distribution (Olch et al., 2014). During treatment procedures, patients are made to lie on a treatment couch in prone or supine anatomical positions (commonly used positions) depending on the region of the target volume. The treatment couch as a support structure offers a reproducible patient positioning, ensuring that the target position and organs are kept constant during the course of the treatment session. Depending on the region being treated, other immobilizing devices are used to further enhance patient positioning. For instance, masks are used to hold the head and neck of the patient in a fixed position and cradles help to hold the patient's body in a fixed position.

These devices usually have effect on the beam parameters, therefore the treatment couch and other immobilizing devices for patients going through radiotherapy procedures are often made of materials with low attenuation properties (low Z elements such as carbon) for the photon energies used in the procedure. Carbon fiber has been identified as an ideal material for the construction of patient support structures and a number of independent studies have shown that carbon fiber offers improved radiotranslucency compared to materials such as plastic and wood. Carbon fiber is also a reinforced composite with specific characteristics like high specific strength and elastic modulus (De Ost et al., 1997). Carbon fiber couches are usually prepared in composite form made of flat boards, each containing two carbon fiber plies separated by a layer of filler material (Njeh et al., 2012). The use of the filler adds extra strength to the carbon fibre by introducing a slit between the two sheets of carbon fibre. Studies have shown that the attenuation of high energy photon beams by carbon fiber inserts is insignificant as compared to hardboard, copolyester and polymethylmethacrylat (PMMA) (De Ost et al., 1997, Meara and Langmack, 1998 and Munjal et al., 2006). Lately, low absorption carbon fiber linac couch tops have replaced high absorption couch tops due to their physical properties which include high strength, low density, translucence, practically no sagging at the end with weight and are more favourable for radiation treatment. Therefore, assortments of such carbon fiber couches and inserts are used lately in clinical practice for three dimensional conformal radiotherapy (3DCRT) and intensity modulated radiotherapy (IMRT) treatments. Currently, amongst the three radiotherapy centres in Ghana, Sweden Ghana Medical Center uses a carbon fiber couch in treatment procedures for cancer management. Korle Bu Teaching Hospital uses plywood and Komfo Anokye Teaching Hospital uses plywood with a wire mesh.

Formerly, it was assumed that carbon fiber therapy couch tops were radio transparent due to their low density foam and carbon fiber composition (Roche, Mahou-Lago, & Crabtree, 2014). However, the general assumption that these carbon fiber couches cause negligible beam attenuation have been questioned over the past few years and a number of studies have indicated that there is significant dose modifications due to these devices (Mihaylov et al., 2013). These modifications include decrease in skin sparing, beam attenuation at depth and change in the point of maximum dose (d_{max}) (Roche et al., 2014). Attenuation of photon beam through carbon fiber couch, a study by De Ost et al., 1997 explicitly dealt with the direct incidence of beam on the couch. They reported that if the beam traverses the couch before entering the patients, there is an undesirable change in the distribution of dose which is not noticeable by the TPS, as most of the commercially available ones have ignored the absorption of beam for posterior oblique incidence of beam. Attenuation by the couch and immobilization devices are major contributing factors (De Ost et al., 1997). High absorption couch tops requires constrained gantry angles for coplanar intensity modulated radiotherapy. Gillis S. et al (2005) reported that for a standard carbon fiber couch, gantry angle is dependent on attenuation measurements. Hence there is the need to account for these errors and incorporate into the treatment planning system.

1.2 STATEMENT OF PROBLEM

Radiation therapy is the most used treatment modalities for the management of cancer hence the need for continuous research and investigations into procedures that will guarantee dose-sparing to critical structures and accurate radiation dose to treatment volumes. Also, the use of new accessories requires a thorough investigation into its effects on the relevant beam parameters.

Many treatment planning systems in their operation, conjectures that the treatment couch tops are made from air equivalent material and thus they will produce the same effect as the beam passing through air. For beams traversing the patient directly without passing through the treatment couch, there is no need to factor in the contributions of treatment couch on the dose and the dose distribution. However, if beams traverse the treatment couch through posterior or posterior oblique directions before reaching the target, the delivered dose to the patient would be less than the planned one. Therefore there is the need to account for the treatment couch's impact on the deposited dose making use of a couch top model in a treatment planning system.

"Owing to studies recommending the consideration of the treatment couch in treatment planning process, investigations are made to factor the couch in the treatment planning system" (Wagner and Vorwerk, 2011). However, most commercial TPSs do not consider beam attenuation. In 2003, a 2-dimensional quantitative study was performed by Vieira et al., 2003 by using an electronic portal imaging device to determine the influence of the treatment couch's components on photon beam attenuation in the course of head and neck treatments, in which they detected up to 15% attenuation of a 6 MV photon beam. It is evident from the study that neglecting the treatment couch during treatment planning process causes the dose distribution at the isocenter to vary, resulting from beam perturbation owing to the presence of couch rails or carbon fiber couch top at certain gantry angles.

The problem is to investigate if the Oncentra MasterPlan TPS v4.3 used for planning patient treatment on the linac at Sweden Ghana Medical Centre, Accra, takes into account the attenuations from the posterior beams. Since if it doesn't, may lead to under dosage of the target tumour.

1.3 OBJECTIVES

The aim of this study is to find out if the Oncentra MasterPlan TPS v4.3 accounts for the attenuations from the posterior beams. It also seeks to probe into the effect of the treatment couch used at SGMC on the dose deposited inside the patient during 3D CRT planning as well as analyse its influence on clinical dose distribution.

These findings will be used to analyse the TPS monitor unit (MU) during dose calculation where the TPS has ignored the presence of the couch in its calculation.

The specific objectives of this the study is:

- Analyse the composition of the couch used for CT dose simulation
- Determine the couch attenuation factors for low and high energy beams for various posterior gantry angles for various field sizes.
- Determine the TPS calculated doses to the compare them to the ion chamber measured doses.
- Model these dose difference into the TPS
- Validate the modeled parameters using an anthropomorphic phantom.
- Implement these into the clinical environment

- Make appropriate recommendations from these findings.

1.4 RELEVANCE AND JUSTIFICATION

Modeling, validating and implementing the carbon fiber treatment couch in treatment planning systems will ensure that the attenuation properties of the couch and its effect on the dose distribution in the patient are accounted for, and hence corrected for by the treatment planning system. This will enhance the degree of confidence in the accuracy of the treatment planning system algorithm for dose calculations and in patient care during cancer management.

1.5 SCOPE AND LIMITATIONS

This research covers these steps:

- CT Scanning of the couch top to determine its homogeneity.
- Acquisition of CT scanned (axial) images of a PMMA phantom to symbolize a patient. The acquired CT images will be loaded into the Oncentra TPS and planned with 6 and 15 MV photon beams for a set of field sizes with varying gantry angles.
- Doses to isocenter for beams going through the couch at various gantry angles compared (for attenuation) with their respective to gantry angles transmitting through air into the phantom.
- The same treatment plan was used on the Linac and measurements taken with a calibrated ion chamber and electrometer.
- Attenuation factors and attenuation correction factors will be calculated for these measurements.
- The treatment couch top was modeled into the Oncentra MasterPlan treatment planning system to quantify the agreement between dose calculated and dose measured.

1.6 ORGANIZATION OF THESIS

Chapter one deals with the background of the study, the problem statement, objectives, relevance of the study, and the scope and limitation. Chapter two contains literature review relevant to the research work. Chapter three describes the research material and methods executed to conduct the study. In chapter three, the experimental procedure for attenuation measurement for varying field sizes and gantry angles are elucidated. In Chapter four, the experimental results and discussion have been presented. Chapter five presents the summary, conclusions as well as recommendations and suggestions for further studies.

CHAPTER TWO

LITERATURE REVIEW

2.1 BACKGROUND

Radiotherapy is one of the treatment modalities for the management of cancer amongst chemotherapy and surgery. Cancerous cells are malignant cells which rapidly proliferate and invade other normal tissues. However, a tumour could be benign and self-contained but may exert some form of pressure on blood vessels and can thereby interrupt normal body functions and cause discomfort. The choice of modality to remove a tumour is determined by the location and mass of the tumour. After the discovery of X-rays by Roentgen in 1895, having aimed at X-ray production technologies to generate higher electron and photon beam energies and intensities, H.E. Johns invented Co-60 teletherapy unit in the early 1950s (Podgorsak & Hendry, 2005). This unit provided higher photon energies until the linear accelerator was invented. Radiotherapy deploys higher energy photons or particulate radiations to destroy cancerous cells in any part of the human body. Since the radiation beam is aimed at a definite area during treatments, most scholars refer to radiotherapy as a local painless treatment (Khan, 2010 and Bushberg et al., 2001). The tumour is damage done by targeting the DNA where cell growth occurs but normal tissues surrounding the target volume are not spared. However, cancerous cells are more prone to destruction compared to normal cells owing to their high proliferating rate and low ability to repair itself (Podgorsak & Hendry, 2005).

2.2 EXTERNAL BEAM RADIATION THERAPY (EBRT)

External beam radiation therapy is a treatment procedure in which high energy beams are directed towards the patient's tumour from a distance. These beams are usually produced outside the body of the patient by linear accelerators or teletherapy cobalt-60 units. EBRT is used for the treatment of deep rooted cancers with the aim of curing the tumour or preventing it from reoccurring. This treatment procedure may be used alone or together with surgery, chemotherapy and even brachytherapy. It is performed prior to surgery to shrink the tumour and make it accessible for removal or after surgery to eliminate those that have infiltrated into the lymph nodes, blood vessels and some other tissues. Sometimes EBRT is used in palliative cases where the cancer is in its advanced stages with the intention of relieving patient from severe pain and other symptoms instead of curing the cancer. Patients receive treatment usually at the outpatient department (OPD) once daily throughout the week for about two to nine weeks depending on the patient diagnosis and the mode of delivery e.g. intensity modulated radiotherapy (IMRT). Before treatment delivery, patient simulation and planning are done. The reason for simulation is to acquire the treatment position that will be used daily during treatment delivery. This position must satisfy both the patient and the radiotherapist such that the patient will be comfortable enough to maintain that position throughout the treatment session with the region of interest accessible for treatment. Simulation is also done to acquire the salient images needed for treatment planning using dedicated X-ray machine or CT scanner. Positioning and immobilisation devices are used to set up and hold patients in a specific position plus the use of permanent marks and tattoos during simulation to obtain images of the treatment area. These marks, tattoos and devices guide to set up patients for daily treatment. The images obtained are then loaded into a treatment planning system where specialised computer program is used to calculate the radiation dose which will be delivered to the tumour and its neighbouring tissue. To obtain an effective treatment outcome, there is the need for the development of a treatment plan that will deliver the apt dose to the tumour while sparing or minimising dose to normal tissues. Over the previous years, treatment delivery techniques have been generated and there has been some series of evolution in these treatment techniques.

2.2.1 The Evolution of Treatment Delivery for EBRT

In the quest to further reduce potential risk of radiation treatment, modern radiation planning techniques have been developed and adopted. These are usually computer assisted with sophisticated tools powerful enough to produce three-dimensional (3D) images of tumours and the use of portal images. Image guided, as well as adaptive radiotherapy techniques, have been used to obtain accurate treatment delivery thereby yielding effective results (Barrett et al., 2009).

The use of radiation to treat cancers begun in the early 20th century with most cases being superficial and were treated without sophisticated machines (Podgorsak & Hendry, 2005). As technology progressed over the years, there was an emergence of a 2-dimensional imaging technique. This technique employs X-ray images to locate the region of the cancer relative to surrounding bony landmarks to avoid irradiating normal tissues during the treatment of cancer cells. In the 1970s – 1980s, CT scanner was developed and this caused a shift from 2-D planning to 3-D planning. 2-D images are reconstructed to obtain a 3-D image or better still a volume of the tumour hence the radiation can be shaped to the tumour size to achieve a good conformality leading to 3-D conformal radiotherapy. Relating the radiation dose to the exact dimensions of the tumour volume allows a higher dose delivery to the tumour while limiting that to surrounding normal tissues. 3-D conformal RT is best for irregular shape tumours or tumours that are closer to healthy tissues and organs.

3-D planning makes use of CT scans and sometimes combined with other imaging modalities such as MRI or PET. PET/CT shows both anatomical and physiological view of the body in a computerised 3-D model. About four to five beams are then oriented around the body such that they all intersect at the target to deliver higher dose to the target and low dose to the surrounding structures.

For more accurate tumour delineation, Intensity Modulated Radiation Therapy IMRT was introduced. IMRT is a treatment delivery procedure that further divides each individual beam into beamlets using small leaves called multi-leaf collimators (MLC's) that move across the path of the beam at diverse speeds and patterns with the beam on as well as varying the gantry angles (Marcu et al., 2012). Therefore, some portions of the radiation beam are intentionally blocked for some time even though treatment is on-going resulting in a higher dose delivery in certain regions and lower dose delivery in other regions. Thus, the intensity across the beam can be modulated hence intensity modulated radiation therapy. It creates a more complex dose distribution around the target by combining about seven to nine of such beams oriented at different angles. Plans are produced in geometric shapes around the target and so critical structures are easily avoided. IMRT can be delivered using dynamic MLC or tomotherapy, step-and-shoot, dose compensation and multiple static fields (Jolly, 2009 & Varian, 2012).

On the other hand, image guided radiotherapy (IGRT) is a delivery technique that allows you to locate and track the tumour in real time of treatment delivery as well as make necessary adjustments whenever there is a tumour shift outside the planned treatment area (Varian, 2012). Tumours have the ability to move thus, organ motion during treatment especially those situated around the lungs and the pelvic areas as a result of breathing, movement of the bladder and the contraction and relaxation of the bowels is inevitable. Therefore, this technology helps to minimise dose to normal tissues and reduce side effects of radiation treatment like skin changes, nausea, fatigue and other symptoms. However, this technique prolongs the overall treatment time.

Adaptive radiotherapy (ART) is also a technique that is used when there is/are regular changes, based on analysis of images taken during or before treatment, to the treatment delivery for an individual patient. And it is done daily or weekly so long as there has been a change in image.

Stereotactic radiotherapy is primarily used for the treatment of small brain tumours and arteriovenous malformations. This technique is very sensitive such that, a stereotactic frame is often used to immobilise the patient's head to an accuracy level of 1 mm for reproducibility sake since there may be several fractions of treatment delivery or may be considered as an alternative to surgery.

2.3 PHOTON INTERACTIONS WITH MATTER

An electromagnetic wave of mass and charge zero is known as a photon. Photons are prone to interact with matter as they move through a medium. Their interactions are basically with electrons or the nucleus of an atom. These interactions could cause short-term or long-lasting damage to the incident particle, target or both. Scattering interactions are reliant on the density of the electron cloud surrounding an atom which is best described by the atomic number (Z) of the medium (Lamarsh & Baratta, 2001). Higher Z materials are known for their high absorption and attenuation properties. Photon interactions largely results in photoelectric effect, pair production, Compton effect, Raleigh scattering as well as photonuclear interactions whenever they pass through a medium. The first three effects are the most significant interactions

(Attix, 1986).

Photoelectric effect takes place when an incident photon of low energy is completely absorbed by an electron leading to the ejection of a photoelectron from the inmost shell of the atom. It is dependent on atomic number such that absorption occurs when a low energy photon moves through a medium of high atomic number.

Pair production is dependent on the incident photon's energy. It occurs when a photon with at least 1.02 MeV energy interacts with the vicinity of the nucleus of an atom to create an electron pair (negatron and positron) with a rest mass of 0.51 MeV each. An increase in the probability of its occurrence is determined by the square of the atomic number (Z) of the material.

Compton effect is an elastic scattering which occurs when a higher energy photon incident on an utmost shell electron and transfers a portion of its energy to the electron before both (photon and electron) are scattered into the medium. The photon is scattered with a higher energy so it has sufficient energy to cause further scattering in another atom. Its occurrence increases linearly with the material's atomic number.

The basic interaction of photons with matter as described above results in the emission of secondary charged particles into the medium. As such, photons are classified as indirectly ionising radiation where a high energy photon causes the release of an electron as it navigates a medium. The photon then transfers its energy to the electron which consequently interacts with and transfers the energy to neighbouring particles (Khan 2010). In external photon beam radiotherapy, 4 to 25 MV photon energies are mostly used (Podgorsak & Hendry, 2005). Again considering the lower atomic number for tissue (~7.5), Compton scattering is the main process of tissue interaction for megavoltage beams. It is directly proportional to electron density in the incident medium (Turner, 2007). As the photon beam strikes the patient surface and traverses through the tissue, the intensity of the beam drops due to the scattering of photons and energy lost to recoil electrons. Fewer high-energy photons are able to reach deeper depths meaning that, the number of electrons released in the medium decreases with increasing depth.

Therefore in EBRT, a photon beam enters the skin and continues to move until it hits a loosely bound electron in a cell. The photon transfers a portion of its energy to the electron and is scattered at an angle relative to its original path. This continues until the photon attains a minimum energy equal to the binding energy of an innermost electron which is then lost by photoelectric interaction.

2.4 CT SIMULATION AND DOSE PLANNING

One most important stage in treatment planning is computer planning and dose calculation. Prior to that, a dedicated CT scanner is used to gather information about the patient's body shapes, healthy organs and the location of the lesion in image form. CT provides an ideal density data for correcting dose for tissue inhomogeneity. The images are then imported onto a treatment planning computer usually known as a treatment planning system TPS. The radiation oncologist uses the TPS to outline specific areas he wants to have treated as well as any normal vital structures which may be influenced by the radiation. Once all areas are designated, a 3 dimensional reconstruction is performed and appropriate radiation fields are added with suitable blocking where applicable to exclude as much normal tissue as possible. The dose calculations are then made to check the dose distribution around the target tissue, the organs at risk and/or normal tissues.

2.5 DOSIMETRIC EFFECTS ON POSITIONING AND IMMOBILISATION DEVICE

In the course of executing treatment procedures of certain tumours in areas such as lip, buccal mucosa, head and neck, it may be advantageous to put an object (wedge, tray or block) across the path of the beam. The object is called a Compensator if it isn't in contact with the surface of the skin at the region of interest (ROI) or a Bolus if it is in contact with the skin at the ROI. Immobilisation devices and beam modifiers are common techniques used to modify isodose curve which optimises target dose distribution (Saffarl & Ghavannasari, 2004). For the sake of reproducibility of treatment procedures, positioning of patient is the most vital and it poses major uncertainties in dose delivery. Therefore, patient set up must be accurate and reproducible each day taking into consideration the stability and comfort of patients as well as minimisation of patient movement. Immobilisation devices on the other hand, provide to certain extent, restriction of movement of ROI and they help maintain patients in a non-standard position from simulation to treatment planning, treatment and from one treatment to another. However the use of these positioning and immobilisation devices cause attenuation in the beam and increase the patient's surface dose. Hence the dosimetric effect of these devices should be assessed carefully.

2.5.1 Impact of Couch Tops on Skin Dose

The surface skin layer is the initial place to exhibit any damage from radiation exposure. During the early days of radiotherapy, before the institution of the Roentgen as the standard unit for radiation exposure, therapists used skin erythema dose (Khan, 2010) as a dosimeter to determine the amount of radiation exposure required to induce skin reddening after exposure (skin dose- response). This unit, however, was discarded based on the fact that reactions of cells to radiation exposure are dependent on factors such as; the amount of radiation, rate of exposure, extent of exposure, and the quality of the beam used for exposure (Bushberg et al., 2001). The pathophysiology, anatomy and skin-dose response have been studied by Archambeau et al., (1995) describing the changes that occur regarding the hair on skin observed clinically as a function of fraction size and total dose such that about 25 Gy at 2 Gy per fraction and over of skin doses causes skin reactions that are clinically and more than 45 Gy may produce dry desquamation. In clinical situations, skin doses are high at areas where the skin folds, bolus are put on surfaces of patients and when electron or orthovoltage beams are used. However, the impact of couch tops and immobilization devices is often not well acknowledged. Kry et al. presented an appraisal of all aspects influencing skin dose in radiotherapy (Kry et al., 2012).

A number of reports has shown a considerable increase in surface dose when beams first transit the couch tops at posterior and posterior oblique angles of incidence and these results are greater as compared to the mylar-covered tennis racket couch top (Seppälä and Kulmala, 2011 and Butson et al., 2007 and De Ost et al., 1997). Literature shows a surface dose of 13% up to 83% for depths up to 0.5 cm for (typically 10 × 10 cm^2) 6 MV X-rays compared to estimates of surface dose of about 16% as reported by various authors in a report compiled by Olch et al., (2014). It also rates the field size dependency on surface dose as significantly greater than that for attenuation. Considering the skin anatomy, Whitton, (1973) reported that the depth of the growing basal cell (sensitive) layer ranges between 0.05 and 0.4 mm, based on anatomical site. The skin dose according to ICRU and ICRP must be measured at 0.07 mm depth, which relates to the estimated depth for the basal cell layer reported by Whitton (ICRU, 1985; ICRU 1991). A reference depth of the basal cell layer of skin often used is 0.1 mm and measurements made at an effective depth greater than this basal layer depth will overrate the skin dose. "Measured doses to the surface for beams traversing a range of thermoplastic and some carbon fiber devices and provided water equivalent thicknesses (WET) and normal tissue complication probability (NTCP) computations of early and late skin damage for 4, 6 and 10 MV photon beams" (Carl and Vestergaard, 2000). . Treatment procedures involving megavoltage beams usually ignore the clinical relevance of skin dose since the main aim is to destroy deep seated tumours.

There was an instance where a higher degree of skin toxicity was recorded in patients undertaking large dose per fraction stereotactic body radiotherapy using three posterior 6 MV beams through the treatment couch top and immobilization device (Figure 2.1). The original plan did not include these devices and recorded about 50% skin dose while subsequent replanning simulating the inclusion of these devices gave a 90% skin dose (Hoppe et al., 2008). This skin reaction was because of a wrong combination of posterior beams, a target volume closer to the skin surface, and other external devices.

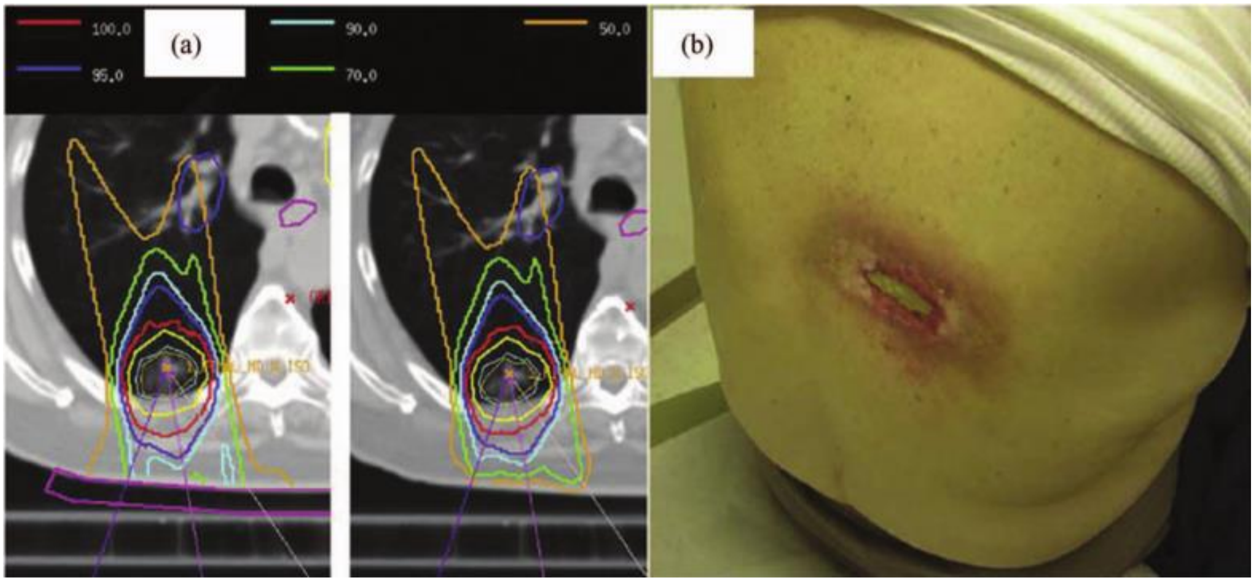

Figure 2.1: (a) (Left panel) Isodoses after including simulated bolus; (right panel) original isodose distribution used to treat the patient. (b) Grade 4 skin reactions (Hoppe et al., 2008).

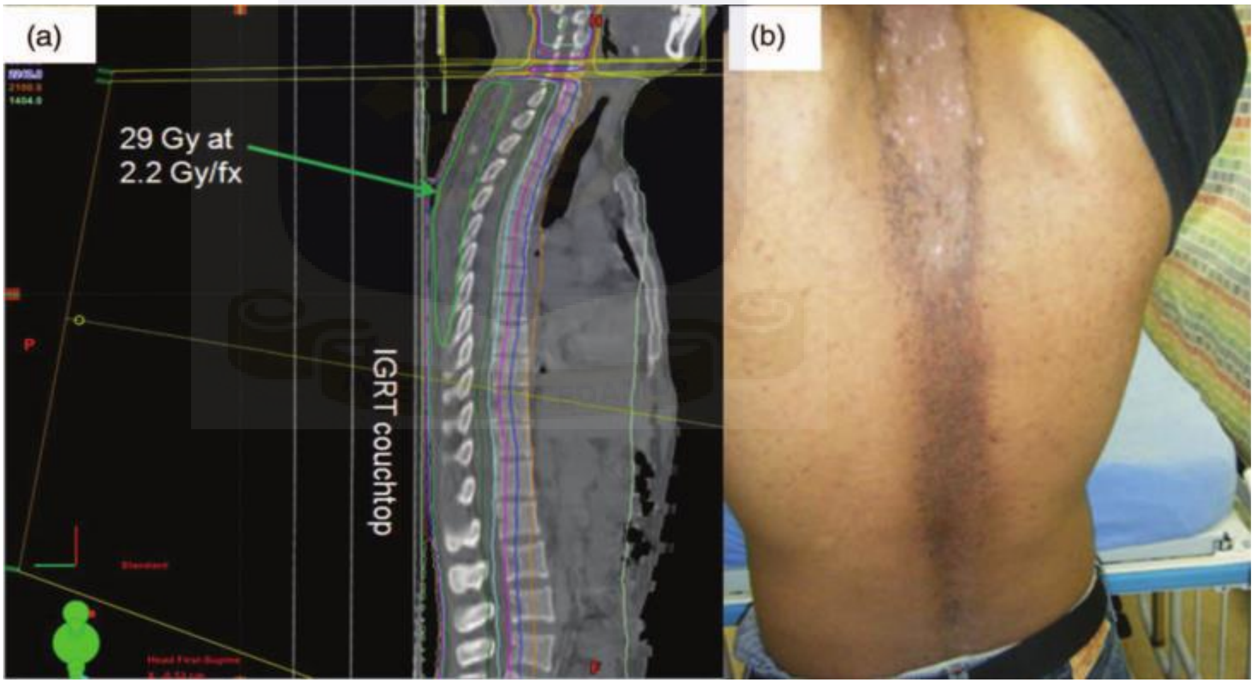

Figure 2.2: (a) PA spine used in craniospinal irradiation (b) Skin reaction from treatment in (a) (Olch et al., 2014).

"A medulloblastoma patient being treated supine on an IGRT couch top with a prescribed dose of 23.4 Gy in 1.8 Gy fractions to the craniospinal axis, a depth of 5 cm using a PA field, obtained a grade 2–3 skin reaction at the back (which was more prominent at the superior aspect of the spine field) after treatment as shown in figure 2.2" (Olch et al., 2014). The maximum superficial dose from the treatment was ≥29 Gy (2.2 Gy/fraction) and much of the increased skin dose was due to treatment through the carbon fiber couch top. In this case, the planning system predicted a high dose region corresponding to the region of the worst aspect of the skin reaction superiorly but placed it at about 1 cm below the skin surface because the couch top was ignored. However, in the first scenario, the planner would have had ample reason to question the safety of the skin dose if the intervening devices were included in the TPS dose calculation but those devices were ignored. It is worth noting that an increase in MU for the correction of couch attenuation has a proportional effect on skin dose. Moreover both energy and field size has an influence on skin dose. "The surface dose is increased from about 10%–60% for 6 MV and 15%–75% for 18 MV (a 50%–60% absolute dose increase) for a 10 × 10 cm^2 field size with and without the carbon fiber couch top" (Meydanci and Kemikler, 2008). Seppala and Kulmala, 2011 also measured the surface dose associated with 8 different couch tops for 6 MV and 15 MV photons for 10×10 cm^2 and 20×20 cm^2 field sizes. Results showed that, depending on the type of couch top, surface doses for a 10 × 10 cm^2 field increased by 26%–37.4% (absolute) for 6 MV and 20% to 43.5% (absolute) for 15 MV photons.

2.5.2 Impact of Couch Tops on Attenuation

The use of patient support (couch) and other immobilisation devices during treatment procedure also attenuate the photon beam apart from increasing skin dose. ICRU seeks to highly conform dose distributions to the target while reducing dose to normal tissues as low as possible by using the most optimal treatment plan. This optimal plan largely depends on the incident beams due to the gantry and couch rotations (Njeh, Raines, & Saunders, 2009). The effect of gantry angle on megavoltage photon beam attenuation by a carbon fiber couch insert has been studied by McCormack et al. where they concluded that the carbon fiber insert can significantly attenuate the radiation beam by 8.7% at an angle of 70°. (McCormack, Diffey, & Morgan, 2005)

Hardboard, copolyester and polymethylmethacrylate PMMA couch inserts that has a high atomic number, Z center spine or side rails presented most attenuating portion as compared to the carbon fibre couch, a study by Krithivas and Rao, 1988. Their study showed an 8%-12% in dose reduction at 60° posterior when a Clinac 4/100 couch was used. Attenuation up to 15% has been identified for certain parts of a modern carbon fiber couch tops. Myint et al., (2006) showed about a 1% difference in attenuation for 6 MV for 5 x 5 cm^2 versus 10 x 10 cm^2 when the magnitude of attenuation was 7% (through a strut). Other reports have shown a 4-fold increase in couch attenuation for beam angles ranging from 0° to 70°. McCormack et al., (2005) pointed out that correcting the central axis dose manually for attenuation may cause an overdose or under dose to regions of the patient where the beam transited a different part of the couch top.

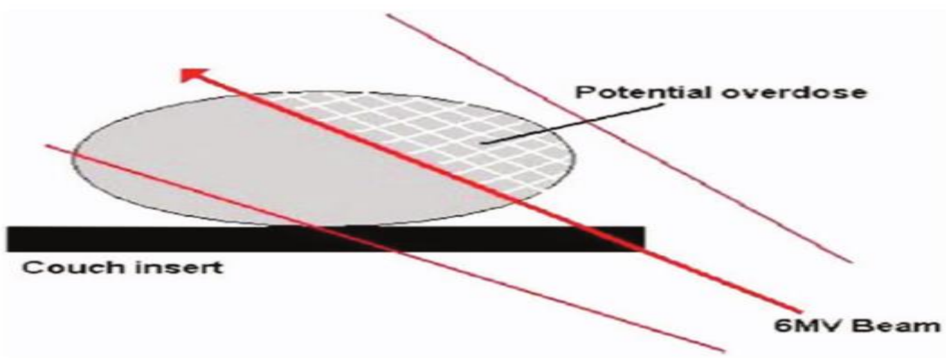

Figure 2.3: Dose perturbation for a 6 MV beam oblique to couch top (McCormack et al., 2005).

Couch top attenuation changes as a function of beam angle has been shown. For 6 MV, attenuation of 1.2%–3.4% and 3.1%–8% was found for normal or 60° beam incidence, respectively.

2.5.3 Impact of the Combination of Couch Tops and Immobilization devices

The accuracy of treatment delivery is critically based on the ability to reproduce patient position throughout the session. There are varieties of patient immobilization equipment on hand to assist in positioning reproducibility. According to Grills et al. (2005) and Rotondo et al. (2008), patient reproducibility can be as good as a few millimetres, which when combined with IGRT can further reduce the inter fraction positioning reproducibility to submillimeter level. However, frequently baseplates or similar devices often made of carbon fiber, plastic, or aluminium are used to connect couch tops to immobilization devices so there is increased in skin dose and attenuation with a magnitude dependent on the type and composition of the device. There is a greater dosimetric effects on the combination of the immobilization devices and couch tops than either alone and both must be considered as a unit in the calculation of dose. The couch and the additional material of the immobilization devices greatly reduce skin sparing due to the beam passing through it (Chiu-Tsao & Chan, 2010). Others reported "attenuation effects up to 11% from the combination of couch and immobilization devices including body and head frames used for stereotactic radiosurgery" (Njeh et al., 2009 & Becker et al., 2009).

2.6 TREATMENT PLANNING PROHIBITIONS

In spite of the fact that it is optimal to include the impact of treatment couch and other external devices in estimation of dose by the TPS, some TPS are unable to do this.

Therefore a protocol which visualizes the devices in the TPS using beams-eye-view (BEV) methods to avoid beams passing through the dose modifying structures has been adopted (Olch et al., 2014).

For planning CTs that do not include couch structures, other methods can still be used to estimate their adjacent positions to avoid the passing of beams through them. During the applications of these methods however, uncertainties should be allowed in the exact location of the external devices relative to the patient introduced by patient position verification couch shifts.

2.6.1 Couch Top Avoidance

To determine the probability of a beam passing through part of the couch top has been addressed by Muthuswamy (1999) by using analytical methods with acceptable accuracy. Geometrical model such as gantry, couch, and collimator angle, as well as jaw and positions of MLC were all factored to estimate beam ray intersections with the couch top (Beange and Nisbet, 2000). More recently, software approaches using a graphical user interface separate from the TPS have been developed (Buckle, 2005). Beam interactions with parts of the couch top became more obvious ever since IMRT became widely used with an increased number of equally spaced coplanar beams unless this was detected earlier and alterations to the treatment plan are made. In some cases, either frame positions (i.e. rails) were moved or gantry angles were modified to avoid the intersection.

Beam intersections appeared in 63% of the plans, which requires changing of the gantry angle of one or more beams. It was concluded that, rotating two posterior-oblique beams by 10^{o} to avoid the intersection would not affect the dose distributions for a prostate treatment (Meyer et al., 2001). TPS ruler tools can be used to approximate whether or not posterior oblique beams will intersect the couch rails or frames. This is as shown in the figure 2.4, where the Eclipse TPS integration of an Exact couch top under the patient CT for an 8 beam coplanar IMRT plan. There are two posterior oblique beams which potentially intersect the rails. The right edge of the right posterior oblique beam (RPO) is protracted by using the ruler tool to show that it just skims the inside corner of the right side rail or a beams-eye-view can be used.

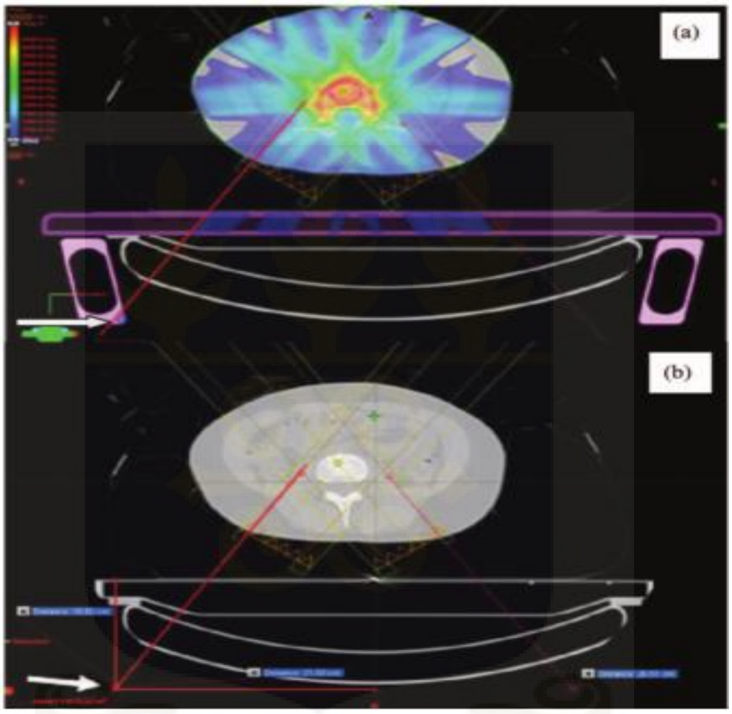

Figure 2.4: (a) Couch is modeled in TPS, (b) couch is not modeled in TPS (Olch et al., 2014).

The figure 2.4 (b) is used when a couch top inclusion feature is not available in the TPS. Here, the height, width and distance from the midline of the couch to the couch rails are measured and the locations of the inner edge of the rail are mapped out using ruler tools. The ruler is used to extend the right edge of the RPO beam to the couch. An additional line is drawn to join the center line of the couch to the known point of the inner part of the right side rail. A third line is drawn downward from the surface of the couch showing the height of the rail. Now, the position of the interior posterior-most corner of the rail has been plotted and the edge of the RPO beam can be placed to avoid it (white arrow). This simple technique works for circumstances where attenuating couch structure geometry is relatively simple and well known. The radiotherapy team must discuss techniques including patient-specific positions, fixed position for all patients with either inclusion of the rails or beam avoidance in the planning process, and the quality assurance implications of each, to determine the choice of rail position.

Also, a portal image of the beam can be used to ascertain to whether or not a beam will pass through an attenuating external structure. Figure 2.5 (a) "shows a PA MV portal image (superior half of field) of a long posterior beam with a large collimator angle used to treat the femur in the frog-legged position, which caused the beam to pass through the solid frame of the couch top" (Olch et al., 2014). Figure 2.5 (b) also shows what this would look like if the plan had been included the couch and frame structure. It can be observed that, the planning process would have anticipated that, the beam would pass through the couch top frame. This situation cannot always be avoided and in such cases, the dosimetric effects of the frame should be evaluated. If the planning system is used to include the couch structure in the calculation, then there will be a change in dose. In cases where the dose decrement is 5% or greater, the external device dose modeling has been validated, the patient is indexed and the daily reproducibility of patient position will be guaranteed, a subfield can also be added to the plan to boost the dose back to 100% just in the region of the attenuating structure (Olch et al., 2014).

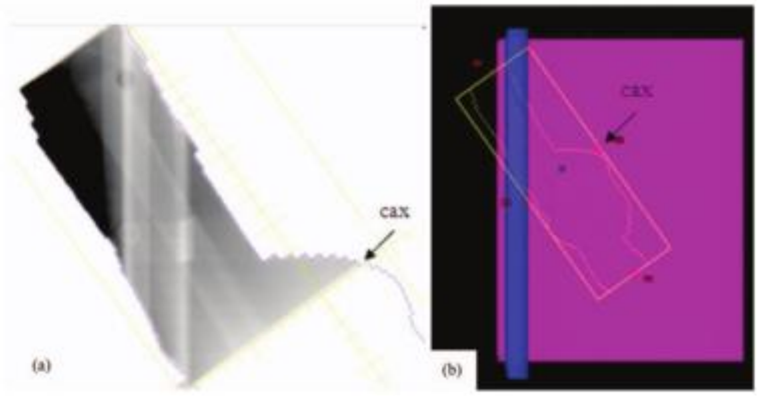

Figure 2.5: (a) EPID image showing couch rail in beam. (b) Rail in beam modeled in TPS (Olch et al., 2014).

2.6.2 Immobilization Device Avoidance

Some TPSs do not account for dose calculations to any structure outside the patient body contour even if it were incorporated and some do not allow divided body contours, which stops the user from contouring the immobilization device as additional "body" volume. However, modern TPSs usually allow contouring and naming any pixel as part of the body contour and will then calculate the dose accordingly. Nevertheless, there is a larger uncertainty associated with the dose calculation and it may be advisable to avoid more attenuating portions of the immobilization devices even if the TPS includes them in the dose calculation (Olch et al., 2014) Visualizing and avoiding immobilization devices is usually forthright since these devices are always in the planning CT images. Some part of the immobilisation devices are often cut off in the planning CT images due to the choice of field of view during imaging. In such cases, the cut off structures should be reintroduced to enhance accurate calculations. The BEV feature in the TPS is used to figure out beam angles which avoid dense structures. An example is as seen in a head fixation system used for brain treatments (Figure 2.6). The BEV shows the vertical post of the head fixation system coinciding with the PTV (red), triggering the beam to pass through this attenuating structure as shown in Figure 2.6 a. By rotating the gantry and/or couch, one can visualize when the beam misses that structure. Contouring external structures helps to avoid external structures in the beam using the BEV method. This method is also useful in VMAT treatments where portions of an arc which would pass through dense external structures can be excluded (Olch et al., 2014).

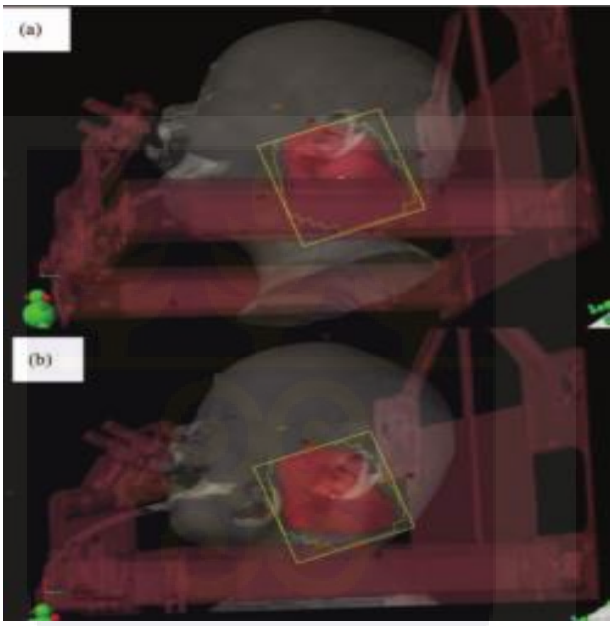

Figure 2.6: (a) BEV of beam intersecting vertical post of immobilization device. (b) Gantry angle changed to avoid the post (Olch et al., 2014).

2.7 DETERMINATION OF ABSORBED DOSE TO WATER UNDER REFERENCE CONDITIONS

The procedure for determining absorbed dose to water is based on the standard of absorbed dose to water as implemented in the national dosimetry recommendations (AAPM, 1999). In most cases, these reference conditions are not met in the clinical settings and this affects the response of the dosimeter (ionization chamber) used in measurement hence the need to distinguish between the reference conditions used in the standard laboratory and the clinical conditions. Reference conditions are influence quantities for which the calibration factor is valid and does not require other correction factors. These influence quantities include; pressure, temperature and polarization voltage which according to TRS 398 may crop up from the dosimeter (e.g. zero drift, ageing warm up) or any parameter related to the radiation field (field size, dose rate, beam quality and depth in a phantom). During calibrations, efforts are made to control these quantities of which most are uncontrollable hence the need for correction using appropriate correction factors (IAEA., 2000). The correction factor of temperature and pressure is applied to convert the cavity air mass in the chamber to that of the reference conditions. The correction factor is given by;

$$k_{TP} = \frac{273.2 + T}{273.2 + T_o} \frac{P_o}{P} \ldots\ldots\ldots\ldots\ldots\ldots\ldots\ldots\ldots\ldots\ldots \quad (2.1)$$

Where: T and P are the cavity air temperature and pressure at time of measurement. T_O and P_O are reference values usually 22°C and 101.3 kPa respectively.

The absorbed dose to water at a reference depth z_{ref} in water for a reference beam quality Q is given by:

$$D_{w,Q} = M_Q N_{D,w,Q_o} k_{QQ_o} \ldots\ldots\ldots\ldots\ldots\ldots\ldots\ldots\ldots (2.2)$$

Where M_Q is the electrometer reading after correction for temperature, pressure, polarity effect and ion recombination. N_{D,w,Q_o} is the calibration factor in term of absorbed dose to water. k_{QQ_o} is the chamber specific factor which corrects for the difference between the reference beam quality and the actual user quality.

2.8 HOUNSFIELD UNIT (HU) SCALE AND CT PROFILE MEASUREMENTS

The Hounsfield Unit (HU) scale is a linear transformation of the linear attenuation coefficient measurement into one in which the radiodensity of distilled water (at standard pressure and temperature) is defined as zero HU, while the radiodensity of air at STP is defined as -1000 HU. For a material X with linear attenuation coefficient μ_x, the HU value is therefore given by the relation:

$$HU = \frac{\mu_x - \mu_{water}}{\mu_{water} - \mu_{air}} \times 1000 \ldots\ldots\ldots\ldots\ldots\ldots\ldots\ldots (2.3)$$

Table 2.1: List of some substances with their HU values

Substance	**HU Values**
Air	-1000
Lung	-500
Water	0
Blood	+30 to +45
Muscle	+10 to +40
Soft Tissue, Contrast	+100 to +300

The mean Hounsfield unit, HU values of the couch can be further converted to electron density relative to water using the equation;

$$\frac{\rho_e}{\rho_{e,w}} = \frac{1 + \text{HU}}{1000} \ldots\ldots\ldots\ldots\ldots\ldots\ldots\ldots\ldots\ldots (2.4)$$

where electron density ρ_e is defined as the number of electrons per unit volume and $\rho_{e,w}$ a linear relationship between HU and is employed over the range of measured HU. The relative electron densities $\frac{\rho_e}{\rho_{e,w}}$ are used to match its corresponding mass densities. A signal intensity profiles relating mass density to relative electron density is used to find the corresponding mass density.

CHAPTER THREE

MATERIALS AND METHODOLOGY

3.1 MATERIALS

The materials used in this research include; Elekta Synergy 11 Platform Linear Accelerator Linac, iBeam evo treatment couch, Polymethylmethacrylat (PMMA) phantom, 0.6cc ionization chamber, PTW UNIDOS electrometer, digital thermometer and barometer, Siemens CT scanner, Oncentra MasterPlan TPS, Male anthropomorphic phantom, Microsoft Excel and MATLAB software.

3.1.1 Elekta Synergy 11 Platform Linear Accelerator

The linear accelerator used at the Sweden Ghana Medical Center for the administration of radiotherapy treatment procedures is the Elekta Synergy 11 Platform (Elekta AB, Stockholm, Sweden) . It was installed in 2011 by Elekta. The purpose of the Elekta Synergy Linac is to produce a beam of high energy electrons or photons for therapeutic use. It is capable of generating two types of clinical beams namely, photon beams which has dual energies of 6 MV and 15 MV and electron beams which has three energies of 6 MeV, 10 MeV and 15 MeV. It has a special multileaf collimator (MLC) of 2 × 40 leaves with a 1 cm leaf width at the isocenter to provide conformal shaping of treatment beams.

3.1.2 iBeam evo Treatment Couch

The iBeam evo Couch top (Elekta AB, Stockholm, Sweden) is used for both CT Simulation and treatment to replicate patient positioning throughout the procedure. It is made up of a homogenous carbon fiber sandwich design which does not contain any metal in the treatment area. This offers improved radiotranslucency hence minimizing attenuation spread across the range of beam entry angles and it provides the perfect solution for IMRT, volumetric arc therapy (VMAT) and image guided radiotherapy (IGRT). Its homogenous construction provides high rigidity and strength and so it has the ability to hold heavy weight without damaging, thus eliminating patient sagging. The iBEAM evo Couch top has an integrated indexing system which optimizes patient positioning accuracy and reproducibility, reducing patient setup time, minimizing patient setup inaccuracies and maximizing the stability of positioning devices.

3.1.3 Polymethylmethacrylat (PMMA) Phantom

The polymethylmethacrylat (PTW, Freiberg, Germany) phantom is an acrylic slab phantom designed for the use of monitor calibrations and quality control measurements within 70 kV up to 50 MV and 1 MeV up to 50 MeV for photon radiation and electron radiation respectively. Each slab phantom consist of 1 plate 1 mm thick, 2 plates each 2 mm thick, 1 plate 5 mm thick and 29 plates each 10 mm thick. This combination makes it possible to vary the measuring depth in additions of 1 mm. The dimension of the whole phantom is 30 cm x 30 cm x 30 cm. In this study, each slab phantom used is 1 cm thick. These slabs provide for backscatter when positioned below the radiation detector (PTW Freiburg, 2012).

3.1.4 PTW Farmer Ionization Chamber

Thimble chambers (PTW, Freiberg, Germany) are best for use in clinical settings because it is convenient, real time (rate or integrated dose), sufficiently sensitive and it is suitable for photon and electron dosimetry. The ionization chamber employed in this study was manufactured by PTW with an active volume of 0.6 cc and a serial number of 000820 (Type 30010). The wall is made of graphite with a protective acrylic cover and the electrode is made of aluminium. The nominal photon energy ranges from 30 KV to 50 MV.

Figure 3.1: PTW Farmer® Ionization Chamber (Type 30010)

3.1.5 PTW UNIDOS^{webline} Electrometer

PTW UNIDOS Electrometer (PTW, Freiberg, Germany) is a solid state type of electrometer used at SGMC. It is mainly used for routine dosimetry measurements where it displays measured values of doses, dose rates and charges after it has been connected to an ionization chamber or any solid state detector in Gy or R, Gy/min or R/min and/or charges/nC. It is a high-precision, secondary standard reference class dosimeter combined with modern network features and offers high quality, reliability and an excellent adaptation to the measuring tasks. The electrometer automatically checks for high voltage between electrodes of the ion chamber in order to prevent damage of the chamber. The device operates on both mains and battery power supply. Air density is corrected by inputting in air pressure and temperature or by means of radioactive check devices. The check device data are stored in a database. UNIDOS^{webline} surpasses the requirements for reference class dosimeters according to IEC60731, the IPEM secondary standard dosimeter guidelines, IEC 61674 for diagnostic radiology and IEC 60846 for health physics (PTW Freiburg, 2012).

Figure 3.2: PTW UNIDOS^{webline} Electrometer

3.1.6 Thermometer and Barometer

The Testo 925 digital thermometer (Testo SE & Co., Maharashtra, India) and the Druck PACE 1000 barometer (GE, Boston, United States) were used in this study to measure the temperature and pressure of the measurement phantoms respectively.

The Testo 925 is known for temperature measurement in heating engineering, the sanitation sector and refrigeration and air conditioning technology hence it is also called *all-rounder* thermometer. It has a thermocouple technology for attachable temperature probes. It enables fast temperature checks and a large temperature measuring range from -50 to +1000 °C (depending on the probe selected).

The Druck PACE 1000 from the Druck standard lab with a serial and certificate number of 3547193 and 0043660 respectively is the barometer used in this study. This pressure indicator is used in pressure measurement for test, calibration and monitoring.

Figure 3.3: Testo 925 Thermometer

Figure 3.4: Druck PACE 1000 Barometer

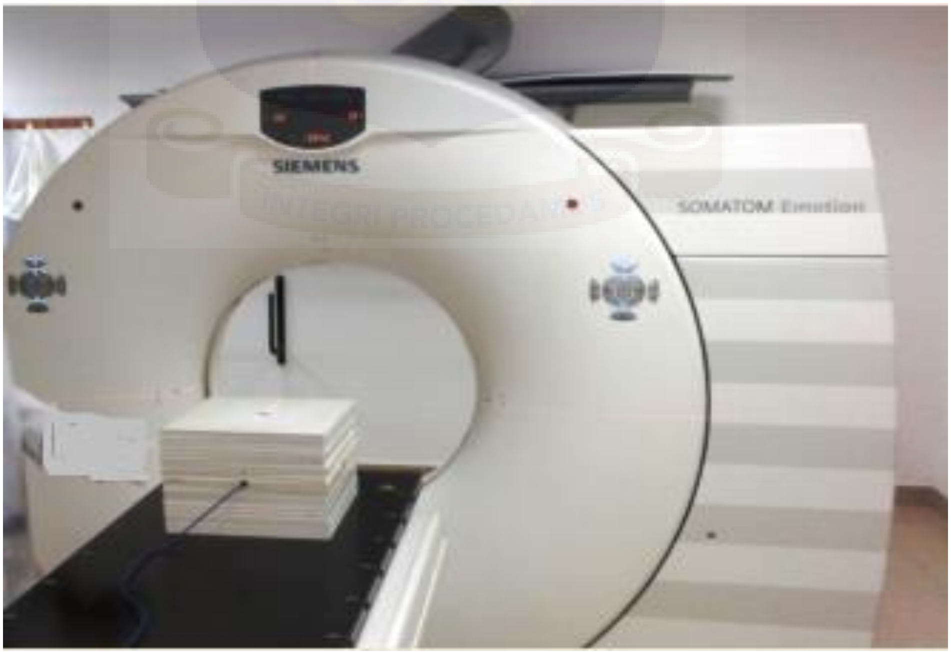

Figure 3.5: Siemen’s 16 slice Somatom Emotion

3.1.7 Siemens CT scanner, Somatom Emotion

The Computerized Tomography (CT) scanner (Siemens Healthineers, Forchheim, Germany) used in this study is a Siemen's 16 slice Somatom Emotion. It has a 16 detector configuration with a focal spot of 0.8x0.5 mm capable of 16x1.2 mm multislice imaging. It has an identification number of 2017BB and installed at SGMC in 2011. The CareDose4D is used as an automatic exposure control feature. This allows automatic adjustment of the tube current in all three dimensions (x, y and z axis) based on the size and area being scanned to obtain a constant image quality. The scanner has tube potentials of 80 KV, 110 KV and 130 KV.

3.1.8 Nucletron Oncentra MasterPlan Treatment Planning System (OMP TPS)

Treatment Planning is the computation method which analyses the energy and fluence for each fundamental beam in order to obtain the dose prescribed to a target volume. As such, the Oncentra system (Nucletron, Columbia, USA) is software designed to analyse and plan radiation treatments in three dimensions. It operates on the Windows© Operating System which a user-friendly interface therefore users easily generate treatment plans for the estimation of dose distributions expected during proposed treatment. The version of the Oncentra MasterPlan used is 4.3. The Oncentra TPS comprises a suite of individual treatment planning modules for external beam radiotherapy and brachytherapy. The modules for the external beam package provide an array of tool for external beam treatment planning using proven physics. The modules include dose calculation algorithms for photon and electron beams such as Collapsed cone and pencil beam for photons and Monte Carlo for electrons. The Collapsed Cone enables the use of Collapsed Cone Convolution algorithm for photon beam dose calculation.

3.1.8 Male anthropomorphic phantom

The anthropomorphic phantom (Long Beach, CA, USA) is well known to be an Alderson Radiation Therapy phantom (ART). They are indispensable quality assurance tool which has been fine tuned in both materials and design. These phantoms are usually made of tissue equivalent materials and are moulded according to ICRU recommendations. The ART phantoms are mostly constructed for male and female. The male anthropomorphic phantom used in this study is 175 cm and 73.5 kg in height and in weight respectively.

3.2 METHODOLOGY

3.2.1 Couch Top Homogeneity Test

The iBeam evo couch top was axially scanned with at tube potential of 110 KV and tube current of 20mAs using the Siemens CT scanner. A topogram of the couch (longitudinal view) was first taken and then axial images of 3mm slice thickness were obtained. An analysis tool that makes use of a circular icon on the graphical user interface calculates the mean CT numbers and standard deviation was used to obtain the mean HU values. The circular icon was placed randomly at left, right and center of each slice of image and mean HU values were recorded. This was repeated on nineteen other slices of image. Mean HU values were recorded and tabulated as shown in Table 1. The aim of this test was to verify the homogeneity of the couch top in terms of its composition.

Figure 3.6: Longitudinal view (right), axial view (left top) of the iBeam evo couch and set up for scanning (left down)

3.2.2 Dose Calculation with Oncentra MasterPlan Treatment Planning System

In order to calculate the absorbed dose deposition using the treatment planning system, a 30x30 cm^2 Perspex PMMA phantom of slabs thickness were arranged to obtain a total of 20 cm. The phantom was placed on the carbon fibre treatment couch and imaged axially using a CT scanner. CT images were generated and then imported to the Oncentra MasterPlan TPS. The images were reconstructed into a three dimensional image as shown in Figure 3.7.

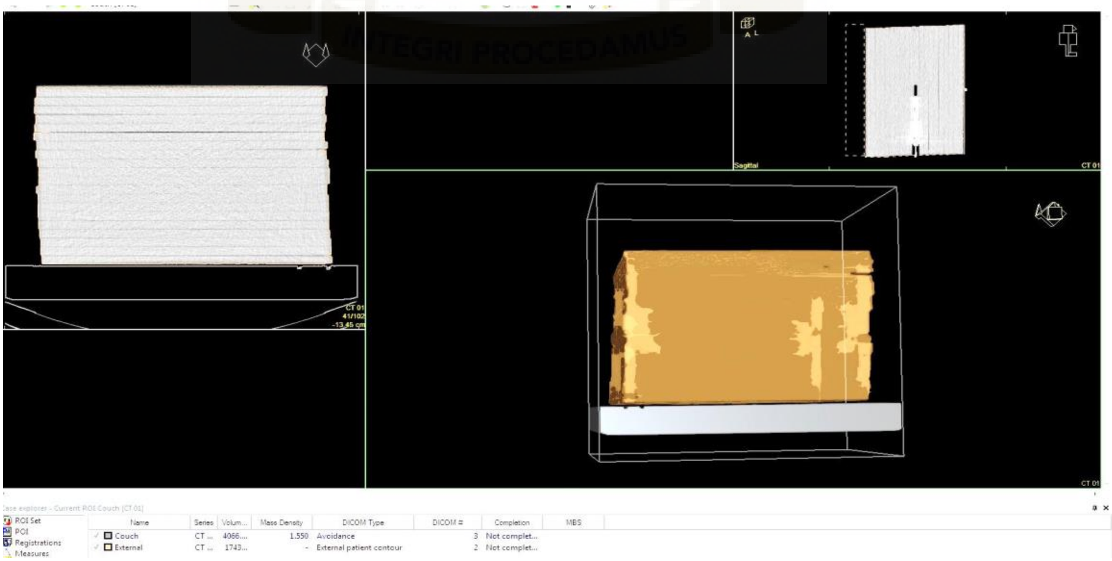

Figure 3.7: TPS interface showing the phantom and the couch top

With the ion chamber already set to the isocenter, a source to axis distance (SAD) of 100 cm and field size of 10×10 cm^2 , a dose of 100 MU was delivered at a depth of 10 cm through varying gantry angles from 0°/360° – 270° anticlockwise and 90° – 180° clockwise rotations. The dose calculation point was put at the isocenter and then calculated using the collapsed cone algorithm and dose reading in Gray (Gy) was recorded. This procedure was done for both 6 and 15 MV photon energies and was repeated for 5×5, 15×15 and 20×20 cm^2 field sizes. The calculated doses were normalized by dividing them by the calculated dose for a 0^o beam angle for a 10×10 cm^2 field size.

3.2.3 Dose measurement with Linac

The 30 cm × 30 cm × 20 cm dimensioned PMMA phantom was used. The middle slab was a 2 cm slab which has an adapter plate to accommodate the ionisation chamber. The ionisation chamber was placed at depth of 10 cm within the phantom as recommended by Olch et al. (2014). The phantom with the ionisation chamber was set up isocentrically on the carbon fibre treatment couch using the alignment lasers. This set up was reproduced from CT images. The ionisation chamber was then connected to the electrometer. The linac was set to deliver a dose of 100 MU. The set up for the study is as shown in Figure 3.8.

Figure 3.8: The experimental set-up showing 0° (right) and 270° (left) gantry angle rotation.

A control console was used to input treatment parameters and execute treatments. The charges (nC) were recorded three times and the average was determined. The initial and final temperature and pressures were also recorded and used to account for temperature and pressure corrections of the ionisation chamber since the chamber is an open system. The ionisation chamber was calibrated at a standard temperature and pressure of 22°C and 101.3 kPa respectively. The correction factor k_{TP} was calculated using equation (2.1). The dose at the reference point was calculated using the TRS 398 Protocol (IAEA., 2000). The average readings were multiplied by the correction factors to obtain the corrected readings. That is:

$$M_{cor} = M_{ave} \times k_{TP} \times k_{pol} \times k_{elec} \times K_S \; \ldots\ldots\ldots\ldots\ldots\ldots\ldots (3.1)$$

Where M_{cor} and M_{ave} are the electrometer reading after corrections for temperature and pressure k_{TP}, polarity effect k_{pol}, electrometerk_{elec} and ion recombination K_S and average electrometer reading respectively. The absorbed dose to water at a reference depth z_{ref} in water for a reference beam quality Q was calculated using equation (2.2).

3.2.3.1 Couch Transmission Factor

The couch transmission factor was determined for field sizes 5×5 cm^2, 10×10 cm^2, 15×15 cm^2 and 20×20 cm^2 using both energies. The readings (charges in nC) were taken for gantry angle 0° such that the radiation beam first traverses the phantom and gantry angle 180° where the beam first incidents the couch. The electrometer readings were then corrected using the correction factors as shown in equations (3.1, 3.2 and 3.3).The transmission factor TF, of the treatment couch was calculated as a ratio of measured value with treatment couch M_{couch} to measured value without treatment couch $M_{no\ couch}$. That is:

$$TF = \frac{M_{couch}}{M_{no\ couch}} \quad \ldots\ldots\ldots\ldots\ldots\ldots\ldots \quad (3.2)$$

3.2.3.2 Relative Attenuation Measurement

Measurements were carried out at gantry angles ranging from 0°/360° to 270° (anterior beam angles with gantry moving anticlockwise) and posterior oblique beam angles from 90° to 180° with 10° gantry interval. Attenuation was calculated as a percentage difference of the dose measured with the couch top in the path of the beam to dose measured without the couch top in the path of the beam. The readings were normalized by dividing them by the reading for 10×10 cm^2 field size at angle 0^o

$$\%\ \text{Attenation} = \left(\frac{D_{0-i} - D_{180-i}}{D_{0-i}}\right) \times 100\,; \qquad i = 10,20,30,40 \ldots\ldots\ldots (3.3)$$

3.2.4 Attenuation Correction Factor

Change in dose with respect to gantry angle can be written as

$$\frac{dD}{d\theta} = -\ \lambda t D \quad \ldots\ldots\ldots\ldots\ldots\ldots\ldots\ldots\ldots \quad (3.4)$$

where $D =$ Dose

$\theta =$ Gantry angle

$\lambda =$ Effective attenuation coefficient

$t =$ Effective Couch thickness

Solving equation (1) using the integrating factor method

$$\frac{dD}{d\theta} + \lambda t D = 0 \quad \ldots\ldots\ldots\ldots\ldots\ldots\ldots\ldots\ldots\ldots (3.5)$$

$$e^{\lambda t}\frac{dD}{d\theta} + \lambda De^{\lambda t} = 0 \ldots \ldots \ldots (3.6)$$

$$\frac{d}{d\theta}\left(De^{\lambda t}\right) = 0 \ldots \ldots \ldots (3.7)$$

$$\int\left[\frac{d}{d\theta}\left(De^{\lambda t}\right)\right]d\theta = c \ldots \ldots \ldots (3.8)$$

$$De^{\lambda t} = c \ldots \ldots \ldots (3.9)$$

$$D = ce^{-\lambda t} \ldots \ldots \ldots (3.10)$$

Let the dose at $\theta = 0$ be D_o where $\lambda = 0$ which implies that

$$D_o = c \ldots \ldots \ldots (3.11)$$

replacing c in equation (2)

$$D = D_o e^{-\lambda t} \ldots \ldots \ldots (3.12)$$

However, the correction factor A is given by the expression

$$A = \frac{D_o}{D} = e^{\lambda t} \ldots \ldots \ldots (3.13)$$

Making λ the subject in equation (4)

$$A = e^{\lambda t} \ldots \ldots \ldots (3.14)$$

$$ln[A] = ln\left[e^{\lambda t}\right] \ldots \ldots \ldots (3.15)$$

$$ln[A] = \lambda t \ldots \ldots \ldots (3.16)$$

$$\lambda = ln[A]\frac{1}{t} \ldots \ldots \ldots (3.17)$$

Using Pythagoras theorem, the couch thickness with respect to gantry angle can be derived as

$$cos\theta = \frac{t_o}{t} \quad => \qquad t = \frac{t_o}{cos\theta} \quad \ldots\ldots\ldots\ldots\ldots\ldots\ldots\ldots\ldots\ldots\ldots\ldots..(3.19)$$

where t_o = Original thickness

then equation (3.14) can be rewritten as

$$\lambda = \frac{cos\theta}{t_o} ln[A] \quad \ldots\ldots\ldots\ldots\ldots\ldots\ldots\ldots\ldots.(3.20)$$

3.2.5 Clinical Validation

In a typical pelvic case, an anthropomorphic phantom was CT scanned and images were imported onto the OMP treatment planning system. For this validation, A 3DCRT Plan and measurements were performed for a standard field size of 10 × 10 cm^2 and a source to surface distance of 100 cm. An AB mimator diode was used as the detector, it had been calibrated to measure dose at a maximum depth, d_{max}, of 1.5 cm and 2.5 cm for photon beam energies 6 MV and 15 MV respectively. The OMP TPS first generated monitor units (MU) of 37.26 for 6 MV and 33.04 for 15 MV, the correction factors were then multiplied by the MUs to obtained corrected MU values which were used to calculate the doses from 120° to 180° gantry angles. The same set up was mounted at the treatment floor where the linac (Elekta Synergy 11 Platform) was used for measurement. Here an AB mimator diode was used to measure the doses for validation. The diodes labelled P10 and P20 represented 6 MV and 15 MV were used for the calibrations and measurements. Now, measurements were made using the corrected MU values obtained for the various gantry angles.

3.2.6 Analysis

Microsoft Excel which forms part of the Microsoft Office 2010 was used to analyse the recorded measurements. The software was used to calculate the average temperature and pressure as well as the average electrometer readings, couch transmission factor and relative attenuation of the couch using equations 3.1, 3.2, 3.3, 3.4 and 3.5 respectively. It was also used in calculating the attenuation correction factor of the iBeam evo couch. A mathematical analysis tool called MATLAB was used to plot graphs used in the data examination.

CHAPTER FOUR

RESULTS AND DISCUSSION

4.1 INTRODUCTION

This chapter presents the results obtained from this study with its discussion. The attenuation factors for both 6 MV and 15 MV photon energies at the various field sizes have been determined. The correction factors have also been obtained and validated.

4.2 COUCH TOP HOMOGENEITY TEST

The iBeam evo couch top was scanned and the measured mean Hounsfield unit (HU) values have been displayed in Table 1 of the appendix. A maximum HU value of -952.3 and a minimum value of -931 were measured and recorded with a deviation of 6.9 HU. These HU values relates to that of air which is -1000 HU. The measured HU values depicted that the couch top was uniformly constructed.

4.3 DOSE CALCULATION WITH ONCENTRA MASTERPLAN TREATMENT PLANNING SYSTEM

The dose deposited to a given calculation point was calculated using the OMP TPS. The calculation point was at a depth of 10 cm and was at the isocenter of the phantom. Two approaches were deployed in calculating the deposited doses using the TPS.

In the first scenario, the couch was incorporated into the TPS and together with the phantom, was treated as one body. And in the second scenario, the incorporated couch and the phantom were contoured as two separate bodies. The calculated doses for all the field sizes and gantry angles at both energies investigated are shown in Appendix B. Results showed equal dose deposition for all field sizes and gantry angles in both scenarios. This implies that the Oncentra MasterPlan TPS depicts the couch as if it were air hence it does not factor it in dose calculation.

There are two ways of accounting for beam attenuation due to the presence of CFC in the beam during treatment delivery. The first is by manually adjusting the TPS monitor units calculation where the TPS has ignored the presence of the couch in its calculation and the second is the incorporation of the CFC into the TPS (Smith et al., 2010). Since the TPS has ignored the presence of the incorporated couch in its dose calculation, further studies was done to manually adjust the monitor units.

4.4 COUCH ATTENUATION FACTOR

The couch attenuation factor was obtained by first determining the transmission factor (TF) of the couch. Using Linac output measurement made with (180^{o} gantry angle) and without (0^{o} gantry angle) carbon fiber couch in the beam, the transmission factor was determined. From physics principles, the sum of reflectance and transmittance of radiation is unity as expressed in Equation in (3.3). Hence the extent to which the 6 MV and 15 MV photon beam is attenuated by the carbon fiber couch was derived. For a 10×10 cm^2 square field, the measured TF was 0.95 and 0.96 for 6 MV and 15 MV photon beam energies and the calculated TF was 1.00 (no attenuation) for both energies. The percentage difference between the measured and calculated TFs 6 MV and 15 MV photon beam energies for a standard field size of 10×10 cm^2 were 5% and 4% at posterior angle. This difference exceeds IAEA recommended tolerance of 2% (IAEA, 2008) when compared with the TF obtained from the TPS.

Table 4.1: Couch AF and TF at various field sizes and energies for Linac output

	Field Size/cm²	Couch/Gy	No Couch/Gy	% TF	% AF
	5 x 5	0.70	0.73	96.20	3.80
	10 x 10	0.79	0.83	95.09	4.91
6 MV	**15 x 15**	0.83	0.85	97.29	2.71
	20 x 20	0.86	0.89	97.57	2.43
	5 x 5	0.81	0.83	97.57	2.43
15 MV	**10 x 10**	0.89	0.92	96.14	3.86
	15 x 15	0.93	0.94	98.43	1.57
	20 x 20	0.96	0.97	98.65	1.35

4.5 TRANSMISSION/ATTENUATION FACTOR DEPENDENCE ON FIELD SIZE, GANTRY ANGLE AND PHOTON ENERGY

On the whole, the attenuation characteristics in relation to the photon energy, field size and the angle of incidence have been studied and they followed anticipated trends. The variation of transmission factor as a function of field size is depicted in Figure 4.1 as a curve. The equation of the correlation is displaced on the curve with its regression (R^2).

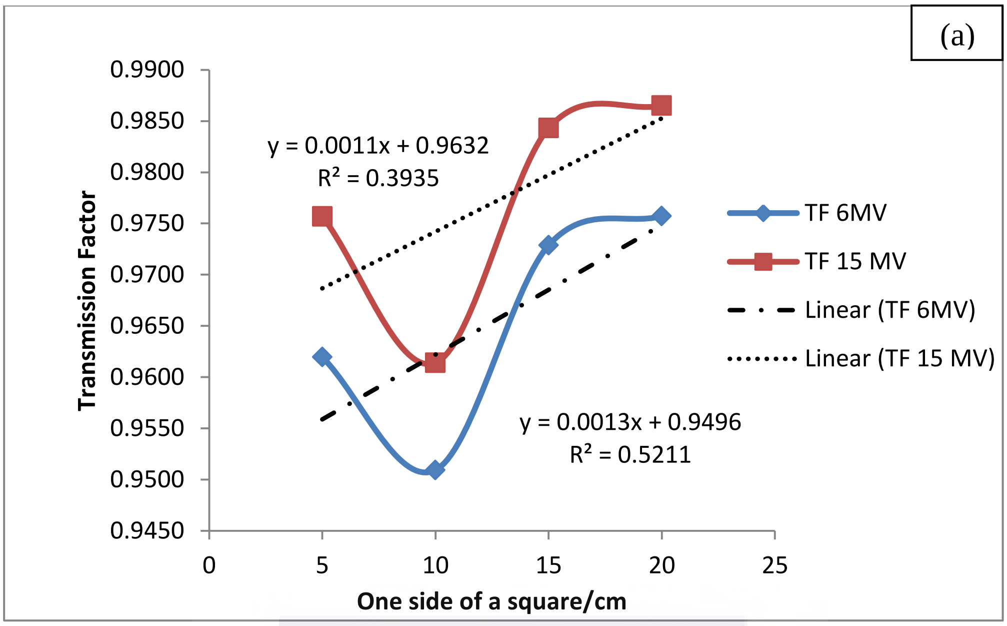

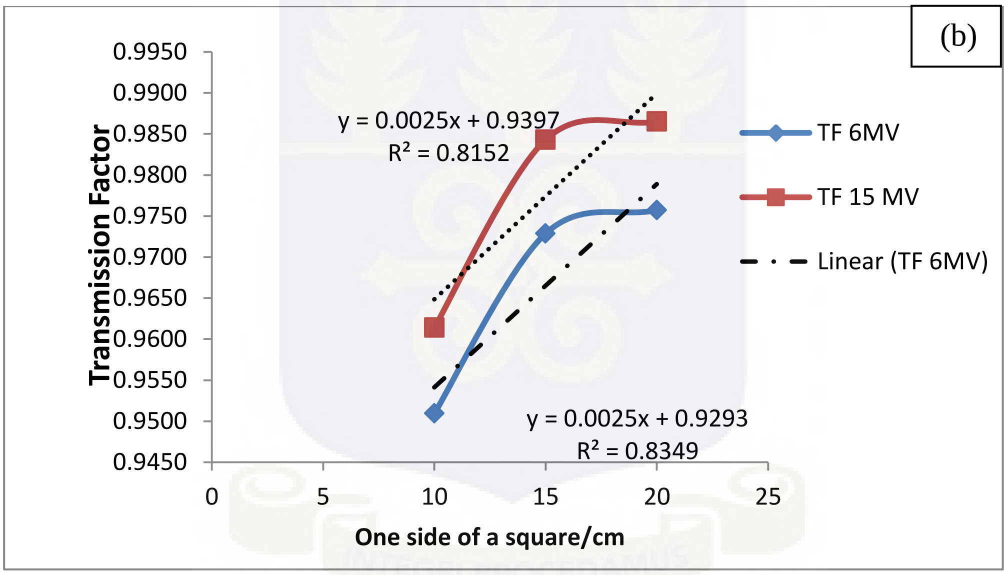

Figure 4.1: A curve showing the variation of transmission factor as a function of field size (a) with and (b) excluding results for the 5×5 cm^2 field size

From Figure 4.1, the transmission factor at 5×5 cm^2 field size for both energies deviates from the usual trend that TF increases with increasing field size. This is due to a phenomenon called small field dosimetry. The curve in (b) shows a rapid increase from 10 cm to 15 cm, then a steady increase from 15 cm to 20 cm without the effect from 5 cm. A higher correlation was obtained in Figure 4.1(b) (R^2 = 0.8349 for 6 MV and 0.8152 for 15 MV) as compared to Figure 4.1(a) where there is a deviation. In terms of fields size dependence, attenuation of 3.8038, 4.9061 2.7131 and 2.4285 for 6 MV and 2.4266, 3.8622, 1.5661 and 1.3529 for 15 MV at field sizes of 5×5 cm^2, 10×10 cm^2, 15×15 cm^2, 20×20 cm^2 respectively. Hence there is a total dependence of transmission factor on field size.

The linear accelerator output has also been observed to vary with gantry angle. Partridge M. et al. (1998) attributed these variations in output measurement to gantry sag, causing slight movements of the electron optics and head components and geometric changes in the beam path. In this study, measurement performed for 10×10 cm^2 field size was used as a reference condition.

As the angle of incidence increases, the path length through which the beam travel within the treatment couch top before striking the surface of the phantom/patients also increases allowing the beam to interact for a longer distance with the couch materials. This causes lesser beam to be transmitted through the couch following the inverse square law. Apparently, it is this same lesser beam that is used in treating patient. This study has shown that the treatment couches have a larger effect on the 6 MV treatment beam as compared to the 15 MV treatment beam, and highest effects for reduced field sizes. Of all the angles of incidence, 130^o was shown to have the highest attenuation. Attenuation of the photon beam is also influenced by the thickness of the carbon fiber used in the construction of the couch. This is clearly demonstrated by the difference in attenuation between the couch (4.91%-7.30%) and (3.86%–5.46%) for both 6 MV and 15 MV but the attenuation rate tends to increase in smaller fields (Table 4.2).

Table 4.2: 6 MV and 15 MV photon beam attenuation dependence on field size and gantry angles

Gantry Angle/°	% Attenuation Factor for 6MV				% Attenuation Factor for 15MV			
Field size/cm^2	5 X 5	10 X 10	15 X 15	20 X 20	5 X 5	10 X 10	15X 15	20X20
180	3.80	4.91	2.71	2.43	2.43	3.86	1.57	1.35
170	3.87	5.07	2.75	2.46	2.37	3.86	1.57	1.36
160	4.23	5.25	2.99	2.60	2.65	4.05	1.71	1.43
150	4.81	5.88	3.34	3.04	2.95	4.33	2.00	1.75
140	5.51	6.27	4.16	3.94	3.56	4.81	2.78	2.51
130	6.69	7.30	5.39	5.01	4.62	5.46	3.61	3.29
120	3.65	5.26	2.99	2.62	2.25	3.93	1.73	1.47
110	0.10	1.69	-0.08	-0.33	-0.08	0.98	-0.45	-0.52
100	-0.25	0.49	-0.38	-0.73	-0.39	0.39	-0.61	-0.76
90	-1.40	-0.13	-1.37	-1.31	-1.26	-0.34	-1.18	-1.18

In the case of energy dependence, there was a lower attenuation by the CFC top at normal incidence for 15 MV compared to 6 MV. As such, most reports limit their study to 6 MV. Meara and Langmack (1998) and Myint et al. (2006) amongst other reports confirm this observation.

4.6 ATTENUATION CORRECTION FACTOR

The effect of CFC tops on photon beam attenuation is an area which needs critical consideration. In this study, approximately 5% and 4% mean dose attenuation was estimated for 6 MV and 15 MV respectively. These values tend to increase with larger field sizes as well as the path length since the effective linear attenuation coefficient is the same due to its homogeneous construction regardless of the gantry angle (Hayashi et al., 2010). Hence it is very necessary to correct the isocenter dose using immobilisation techniques and correction factors.

Gantry angle dependency of attenuation by CFC top in this study was observed between 4.91% and 3.86 (minimum) and 7.3% and 5.46(maximum) at 180° and 130° for 6 MV and 15 MV photon energies at 10×10 cm^2 standard field size, respectively. When the gantry angle changed from 180° to ± 50°, photon beam attenuation increased significantly. The attenuation correction factor for this gantry angle dependency was calculated using equation 3.6 and results is as shown in Figure 4.2 and Figure 4.3 for both energies. The left side of the equation represented the measured values and the right represented the predicted values making use of the new increments in effective couch thickness by a factor of $1/cos\theta$.

The measured values agreed well with the predicted values at angles of incidence of 180° ± 50°, but slightly disagreed at 60° to 70°. The reason being that, the path length at which the photon beam travels (the effective couch thickness) tend to reduce after angle of incidence of 130° during the actual treatment. However, it is presumed in theory that the effective couch thickness keep increasing until a photon beam strikes the surface at an incident angle of 90°.

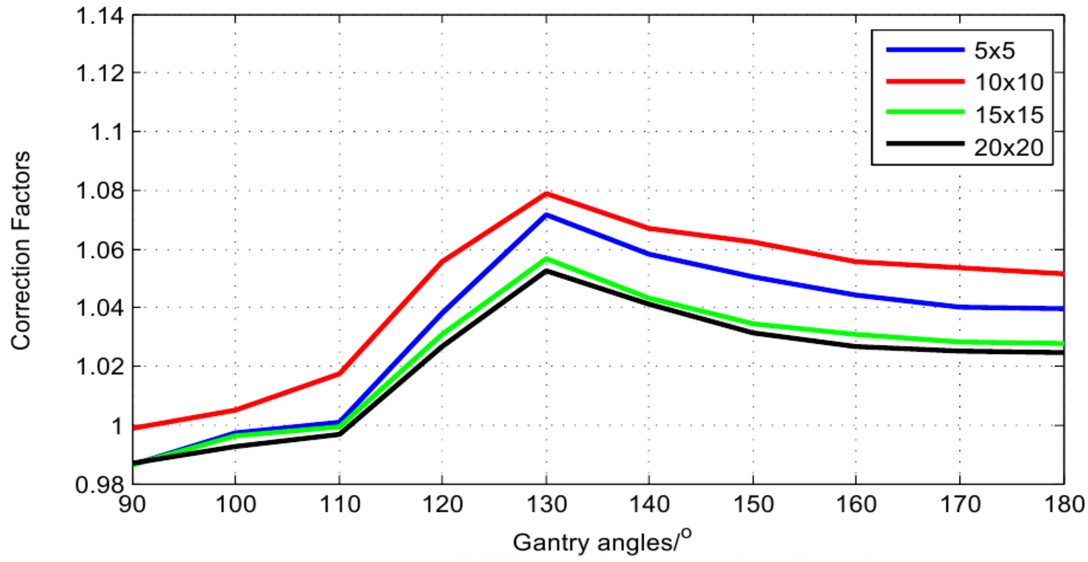

Figure 4. 2: Attenuation correction factors as a function of gantry angles for 6 MV photon beam

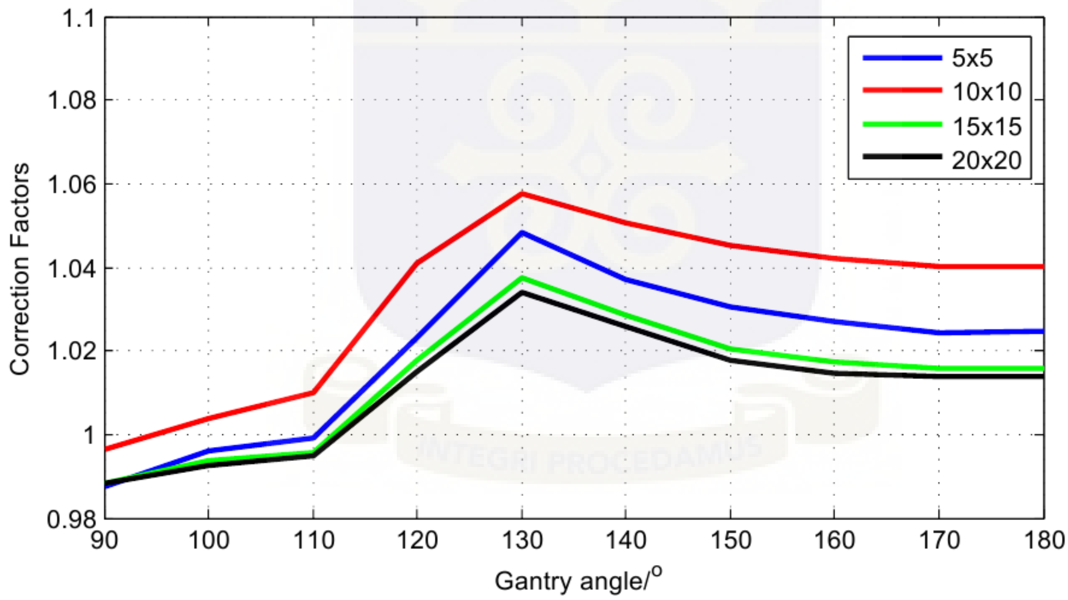

Figure 4. 3: Attenuation correction factors as a function of gantry angles for 15 MV photon beam.

4.7 CLINICAL VALIDATION

The beams passing through CFC top from the gantry angle of 180° to 120° were validated both by the OMP treatment planning system and the Elekta Synergy Platform 11 linac. Using 37.26 MU for 6 MV and 33.04 MU for 15 MV multiplied by the attenuation correction factors at various gantry angle ACF_{θ}, a corresponding dose was calculated by the TPS and the AB mimator diode was used to measure the absorbed dose deposited at the various gantry angles. Inverse square law corrections were done on the planned dose to obtain the actual dose. The percentage deviation between the actual dose to be deposited and the measured dose was up to 7% which is within the acceptable range of ±7% for AB mimator diodes. This is as shown in Appendix E hence the measured absorbed dose showing good agreement with the planned doses.

CHAPTER FIVE

CONCLUSION AND RECOMMENDATION

5.1 CONCLUSION

Treatment of patients using treatment couch tops, immobilisation devices or even a combination of these can alter the dose received by that patient in a clinical setting. Photon beam attenuation by couch top should be considered to deliver the correct dose for cases involving posterior and posterior oblique beams.

This study showed that attenuation values for the iBeam evo carbon fiber couch top increased from 4.9 and 3.86% at normal incidence to 7.3 and 5.36% at oblique incidence of 130° for a 6 MV and 15 MV beam respectively. Similar results were measured for the Civco Universal couch. From these results it was possible to conclude that attenuation due to the couch tops increases as field size is decreased, as energy is decreased and at posterior oblique angles as compared to the results obtained by Roche et al., (2014).

A simple method using the proposed equation and a correction factor should be useful to correct the isocenter dose when the attenuation effect cannot be corrected by the TPS. For beams perpendicular and oblique to a uniform slab, attenuation correction factors can be measured and applied manually to the MU calculation.

5.2 RECOMMENDATION

Below are the recommendations made to the various stakeholders in the treatment of cancer at the Radiotherapy Department of SGMC and the research community.

5.2.1 Clinical Community

It has been established that, it is a possible to model couches in TPSs that does not support couch modeling, therefore it is recommended that more work is done on this subject. Facilities should upgrade to a treatment planning system which has already accounted for the presence of couch in the beam. Regular medical physics audit should be encouraged.

Medical Physicists/ dosimetrists should as much as possible, ignore angles which gave higher attenuation values and also consider the use of small volume detectors for measurements involving small fields. Further work can also be done using other detectors (i.e. Gafchromic film) for verification

Consideration should be given to the impact on skin dose and dose distribution in future works on this topic. It is also recommended that the Radiotherapy Department of SGMC should establish a couch model for all couch inserts in their TPS in order to give good treatment for diseases where beams would have to transit through couches before interacting with the patients.

5.2.2 Regulators and Policy Makers

Regulators and policy makers should ensure that radiotherapy facilities have workable protocols to infuse couch top modeling in their TPS.

REFERENCES

AMERICAN ASSOCIATION OF PHYSICISTS IN MEDICINE, Task Group 51: Protocol for clinical reference dosimetry of high-energy photon and electron beams, Med. Phys. 26 (1999) 1847–1870.

Archambeau, J. O., Pezner, R. and Wasserman, T. (1995). “Pathophysiology of irradiated skin and breast,” Int. J. Radiat. Oncol. Biol., Phys. 31: 1171–1185.

Attix, F. H. (1986). "Introduction to Radiological Physics and Radiation Dosimetry" (Wiley-VCH Verlag GmbH & Co.KGaA).

Barrett, A., Dobbs, J., Morris, S. & Roques, T. (2009).Practical Radiotherapy Planning. Italy: Macmillan Publishing Solutions.

Beange, I. and Nisbet, A., (2000). “A collision prevention software tool for complex three-dimensional isocentric set-ups,” Br. J. Radiol. 73: 537–541.

Becker, S. J., Jozsef, G. and DeWyngaert, J. K. (2009). “Characterization of the transmission of the Elekta Stereotactic Body Frame (ESBF) and accounting for it during treatment planning,” Med. Dosim. 34: 154–157.

Butson, M. J., Cheung, T. and Yu, P. K. N. (2007). “Megavoltage X-ray skin dose variation with an angle using grid carbon fiber couch tops,” Phys. Med. Biol. 52: N485–N492.

Carl, J. and Vestergaard, A. (2000). “Skin damage probabilities using fixation materials in high-energy photon beams,” Radiother. Oncol. 55: 191–198.

Chiu-Tsao, S. T. and Chan, M. F. (2009). “Photon beam dosimetry in the superficial buildup region using radiochromic EBT film stacks,” Med. Phys. 36: 2074–

2083.

De Ost B., Vanregemorter J., Schaeken B. and Van den Weyngaert D. (1997). The effect of carbon fibre inserts on the build-up and attenuation of high energy photon beams. Radiother Oncol, 45(3):275–277.

Gillis, S., Bral, S., De Wagter, C., Derie, C., Paelinck, L., Van Vaerenbergh, K., Coghe, M., De Meerleer, G. and De Neve, W. (2005). “Evaluation of the Sinmed Mastercouch® as replacement for a standard couch,” Radiother. Oncol. 75: 227–236.

Hoppe, B. S., Laser, B., Kowalski, A. V., Fontenla, S. C., Pena-Greenberg, E., Yorke, E. D., Lovelock, D. M., Hunt, M. A. and Rosenzweig, K. E. (2008). “Acute skin toxicity following stereotactic body radiation therapy for stage I nonsmall-cell lung cancer: who’s at risk?” Int. J. Radiat. Oncol., Biol., Phys.72: 1283–1286.

International Atomic Energy Agency (2000). Absorbed Dose Determination in External Beam Radiotherapy: An international code of practice for dosimetry based on standards of absorbed dose to water. Technical Report Series 398. IAEA, Vienna.

Jolly, D., Alahakone, D. and Meyer, J. (2009). "A rapidarc planning strategy for prostate with simultaneous integrated boost" J. Appl. Clin. Med. Phys., 12 (1): 3320.

Kahn, F. M., (2010). "The Physics of Radiation Therapy," 4th ed. (Lippincott Williams & Wilkins, Philadelphia, PA).

Krithivas, G. and Rao, S. N. (1988). "Arc therapy dose perturbation due to the center bar in a Clinac 4/100 couch assembly," Med. Dosim. 13: 15–18.

Kry, S. F., Smith, S. A., Weathers, R. and Stovall, M. (2012). "Skin dose during radiotherapy: a summary and general estimation technique," J. Appl. Clin. Med. Phys. 13: 20–34.

Marcu, L., Bezak, E. and Allen, B. (2012). "Biomedical Physics in Radiotherapy for Cancer" (Springer Science and Business Media B.V., New York).

McCormack, S., Diffey, J., & Morgan, A. (2005). The effect of gantry angle on megavoltage photon beam attenuation by a carbon fiber couch insert. *Medical Physics*, *32*(2), 483– 487. http://doi.org/10.1118/1.1852792

Meara S. J. and Langmack, K. A. (1998). An investigation into the use of carbon fibre for megavoltage radiotherapy applications. Phys Med Biol, 43(5):1359–1366.

Meydanci, T. and Kemikler, G. (2008). "Effect of a carbon fiber tabletop on the surfacedose and attenuation for high-energy photon beams," Radiat. Med. 26, 539–544.

Meyer, J., Mills, J. A. Haas, O. C. L., Burnham, K. J. and Parvin, E. M. (2001). "Accommodation of couch constraints for coplanar intensity modulated radiation therapy," Radiother. Oncol. 61, 23–32.

Mihaylov, I. B., Corry, P., Yan, Y., Ratanatharathorn, V., Moros, E. G., Mihaylov, I. B., Moros, E. G. (2013). Modeling of carbon fiber couch attenuation properties with a commercial treatment planning system Modeling of carbon fiber couch attenuation properties, *4982*(2008).

http://doi.org/10.1118/1.2982135

Munjal, R. K, Negi, P. S., Babu A. G., Sinha, S. N., Anand A. K., and Kataria, (2006) T. Impact of 6MV photon beam attenuation by carbon fiber couch and immobilization devices in IMRT planning and dose delivery. J Med Phys, 31(2):67–71.

Muthuswamy, M. S. (1999). “A method of beam-couch intersection detection,” Med. Phys. 26, 229–235.

Myint, W., K., Niedbala, M., Wilkins, D., Gerig, L.,H. (2006). Investigating treatment dose error due to beam attenuation by a carbon fiber tabletop. J Appl Clin Med Phys. ;7(3):21–27.

Njeh, C. F., Raines, T. W., & Saunders, M. W. (2009). Determination of the photon beam attenuation by the BrainLAB imaging couch : angular and field size dependence, *10*(3): 16–27.

Olch, A. J., Gerig, L., Li, H., Mihaylov, I., Morgan, A., & Gerig, L. (2014). Dosimetric effects caused by couch tops and immobilization devices : Report of AAPM Task Group 176 Dosimetric effects caused by couch tops and immobilization devices : Report of AAPM Task Group 176, *61501*(43). http://doi.org/10.1118/1.4876299

Partridge, M., Evans, P. M. & Mosleh-Shirazi MA. (1998). Linear accelerator output variations and their consequences for megavoltage imaging. Med Phys. 25(8):1443–52.

Podgorsak, E. B. and Hendry, J. H. (2005). "Radiation Oncology Physics: A Handbook for Teachers and Students" (International Atomic Energy Association, Vienna).

PTW Freiburg GmbH. (2012). Dosimetry Solutions for Radiation Therapy. Retrieved from http://www.ptw.de/acrylic_and_rw3_slab_phantoms0.html

PTW Freiburg GmbH. (2012). Dosimetry Solutions for Radiation Therapy. Retrieved from http://www.ptw.de/unidos_e_dosemeter_ad0.html

Roche, M., Mahou-Lago, S. M., & Crabtree, T. (2014). Accounting for the effects of carbon fiber treatment couches in the XiO treatment planning system. *Journal of Physics: Conference Series*, *489*, 12022. http://doi.org/10.1088/1742-6596/489/1/012022

Rotondo,R. L., Sultanem, K., Lavoie,I., Skelly, J. and Raymond, L. (2008). "Comparison of repositioning accuracy of two commercially available immobilization systems for treatment of head-and-neck tumors using simulation computed tomography imaging," Int. J. Radiat. Oncol., Biol., Phys. 70: 1389–1396

Saffar1, M. H., Ghavamnasiri, M.R. (2004) "Assessment of variation of wedge factor with depth, field size and SSD for Neptun 10PC Linac" J. Radiat.; 2 (2): 53-58.

Seppälä, J. K. H., and Kulmala, J. A. J. (2011). "Increased beam attenuation and surface dose by different couch inserts of treatment tables used in megavoltage radiotherapy," J. Appl. Clin. Med. Phys. 12: 15–23.

Smith, D. W., Christophides, D., Dean, C., Naisbit, M., Mason, J., & Morgan, A. (2010). Dosimetric characterization of the iBEAM evo carbon fiber couch for radiotherapy. *Medical Physics*, *37*(7): 3595–3606. http://doi.org/10.1118/1.3451114

Turner, J. E. (2007). "Atoms, Radiation, and Radiation Protection," 3rd ed. (Wiley-VCH, Berlin, Germany).

Varian Medical Systems, Benefits of IGRT, (2012). http://www.varian.com/us/oncology/treatments/treatment_techniques/IGRT/benefits.html

Varian Medical Systems, The Benefits of SmartBeam IMRT (2012). http://www.varian.com/us/oncology/treatments/treatmenttechniques/IMRT/benefits.html

Vieira, S. C., Kaatee, R. S., Dirkx, M. L. and Heijmen, B. J. B. (2003). "Two dimensional measurement of photon beam attenuation by the treatment couch and immobilization devices using an electronic portal imaging device," J. Med. Phys. 30: 2981

Wagner D, Vorwerk H (2011) Treatment Couch Modeling in the Treatment Planning System Eclipse. J Cancer SciTher 3: 007-012. doi:10.4172/1948-5956.1000049

Whitton, J. T. (1973). "New values for epidermal thickness and their importance," Health Phys. 24: 1–8.

APPENDIX

APPENDIX A: Mean HU values of the iBeam evo couch top

Slice No.	Mean HU value	Slice No.	Mean HU value
1	-951.3	11	-949.6
2	-943.5	12	-940.8
3	-939.0	13	-935.9
4	-950.6	14	-951.4
5	-950.5	15	-931.0
6	-948.1	16	-947.5
7	-949.1	17	942.2
8	-940.7	18	-952.3
9	-949.9	19	-942.9
10	-951.1	20	-943.6

APPENDIX B:

APPENDIX B: Dose calculation with Oncentra MasterPlan Treatment Planning System

APPENDIX B 1: 6 MV Photon Energy at 5×5 cm^2

5x5 cm^2					
No Couch			**Couch**		
Gantry Angle/°	**Dose/Gy**	**$N_{DW,Q}$**	**Gantry Angle/°**	**Dose/Gy**	**$N_{DW,Q}$**
0	0.72	0.90	180	0.73	0.91
350	0.72	0.90	170	0.72	0.90
340	0.70	0.88	160	0.70	0.88
330	0.66	0.83	150	0.66	0.83
320	0.60	0.75	140	0.60	0.75
310	0.51	0.64	130	0.51	0.64
300	0.45	0.56	120	0.46	0.58
290	0.49	0.61	110	0.50	0.63
280	0.52	0.65	100	0.53	0.66
270	0.54	0.68	90	0.54	0.68

10x10 cm^2					
No Couch			**Couch**		
Gantry Angle/°	**Dose/Gy**	**$N_{DW,Q}$**	**Gantry Angle/°**	**Dose/Gy**	**$N_{DW,Q}$**
0	0.80	1.00	180	0.80	1.00
350	0.80	1.00	170	0.79	0.99
340	0.77	0.96	160	0.77	0.96
330	0.73	0.91	150	0.73	0.91
320	0.67	0.84	140	0.67	0.84
310	0.58	0.73	130	0.58	0.73
300	0.52	0.65	120	0.52	0.65
290	0.56	0.70	110	0.57	0.71
280	0.59	0.74	100	0.60	0.75
270	0.61	0.76	90	0.61	0.76

15x15 cm^2					
No Couch			Couch		
Gantry Angle/°	Dose/Gy	$N_{DW,Q}$	Gantry Angle/°	Dose/Gy	$N_{DW,Q}$
0	0.85	1.06	180	0.85	1.06
350	0.84	1.05	170	0.84	1.05
340	0.82	1.03	160	0.82	1.03
330	0.78	0.98	150	0.78	0.98
320	0.72	0.90	140	0.72	0.90
310	0.62	0.78	130	0.62	0.78
300	0.56	0.70	120	0.57	0.71
290	0.61	0.76	110	0.62	0.78
280	0.64	0.80	100	0.65	0.81
270	0.66	0.83	90	0.66	0.83

20x20 cm^2					
No Couch			Couch		
Gantry Angle/°	Dose/Gy	$N_{DW,Q}$	Gantry Angle/°	Dose/Gy	$N_{DW,Q}$
0	0.88	1.10	180	0.88	1.10
350	0.87	1.09	170	0.87	1.09
340	0.85	1.06	160	0.85	1.06
330	0.81	1.01	150	0.81	1.01
320	0.75	0.94	140	0.74	0.93
310	0.64	0.80	130	0.65	0.81
300	0.59	0.74	120	0.59	0.74
290	0.63	0.79	110	0.65	0.81
280	0.67	0.84	100	0.68	0.85
270	0.69	0.86	90	0.69	0.86

APPENDIX B 2: 15 MV Photon Energy

5x5 cm^2					
No Couch			Couch		
Gantry Angle/°	Dose/Gy	$N_{DW,Q}$	Gantry Angle/°	Dose/Gy	$N_{DW,Q}$
0	0.83	0.92	180	0.83	0.92
350	0.82	0.91	170	0.82	0.91
340	0.80	0.89	160	0.80	0.89
330	0.77	0.86	150	0.76	0.84
320	0.71	0.79	140	0.70	0.78
310	0.62	0.69	130	0.62	0.69
300	0.57	0.63	120	0.57	0.63
290	0.60	0.67	110	0.62	0.69
280	0.63	0.70	100	0.64	0.71
270	0.65	0.72	90	0.65	0.72

10x10 cm^2					
No Couch			Couch		
Gantry Angle/°	Dose/Gy	$N_{DW,Q}$	Gantry Angle/°	Dose/Gy	$N_{DW,Q}$
0	0.90	1.00	180	0.90	1.00
350	0.89	0.99	170	0.89	0.99
340	0.87	0.97	160	0.87	0.97
330	0.84	0.93	150	0.83	0.92
320	0.78	0.87	140	0.77	0.86
310	0.69	0.77	130	0.68	0.76
300	0.63	0.70	120	0.63	0.70
290	0.67	0.74	110	0.68	0.76
280	0.70	0.78	100	0.71	0.79
270	0.72	0.80	90	0.71	0.79

15x15 cm^2					
No Couch			Couch		
Gantry Angle/°	**Dose/Gy**	**$N_{DW,Q}$**	**Gantry Angle/°**	**Dose/Gy**	**$N_{DW,Q}$**
0	0.94	1.04	180	0.94	1.04
350	0.93	1.03	170	0.93	1.03
340	0.91	1.01	160	0.91	1.01
330	0.88	0.98	150	0.87	0.97
320	0.82	0.91	140	0.81	0.90
310	0.72	0.80	130	0.72	0.80
300	0.67	0.74	120	0.67	0.74
290	0.71	0.79	110	0.72	0.80
280	0.74	0.82	100	0.75	0.83
270	0.76	0.84	90	0.76	0.84

20x20 cm^2					
No Couch			Couch		
Gantry Angle/°	**Dose/Gy**	**$N_{DW,Q}$**	**Gantry Angle/°**	**Dose/Gy**	**$N_{DW,Q}$**
0	0.96	1.07	180	0.96	1.07
350	0.95	1.06	170	0.95	1.06
340	0.93	1.03	160	0.93	1.03
330	0.90	1.00	150	0.89	0.99
320	0.84	0.93	140	0.83	0.92
310	0.74	0.82	130	0.74	0.82
300	0.68	0.76	120	0.68	0.76
290	0.73	0.81	110	0.74	0.82
280	0.76	0.84	100	0.77	0.86
270	0.79	0.88	90	0.78	0.87

APPENDIX C: Raw data measurements showing average Temperature, Pressure and corrected Ionization Chamber readings for Couch TF and Relative Attenuation Measurements

APPENDIX C1: 6 MV Photon Energy

5x5 cm^2							
No Couch							
Gantry Angle/°	**M1/nC**	**M2/nC**	**M3/nC**	**M/nC**	**Mcor / nC**	**DW,Q**	**$N_{DW,Q}$**
0	13.32	13.32	13.32	13.32	13.61	0.73	0.88
350	13.27	13.26	13.26	13.26	13.55	0.73	0.88
340	13.00	13.00	13.00	13.00	13.28	0.71	0.86
330	12.54	12.55	12.55	12.55	12.82	0.69	0.83
320	11.79	11.79	11.79	11.79	12.04	0.65	0.78
310	10.65	10.65	10.65	10.65	10.88	0.58	0.71
300	9.75	9.73	9.75	9.74	9.95	0.53	0.65
290	10.32	10.32	10.32	10.32	10.54	0.57	0.68
280	10.70	10.70	10.70	10.70	10.93	0.59	0.71
270	10.71	10.72	10.72	10.72	10.95	0.59	0.71
Couch							
90	10.86	10.87	10.87	10.87	11.10	0.60	0.72
100	10.72	10.73	10.73	10.73	10.96	0.59	0.71
110	10.31	10.31	10.31	10.31	10.53	0.57	0.68
120	9.38	9.40	9.38	9.38	9.58	0.52	0.62
130	9.93	9.94	9.94	9.94	10.15	0.55	0.66
140	11.14	11.14	11.14	11.14	11.38	0.61	0.74
150	11.94	11.94	11.95	11.94	12.20	0.66	0.79
160	12.45	12.45	12.45	12.45	12.72	0.68	0.83
170	12.75	12.75	12.75	12.75	13.02	0.70	0.85
180	12.83	12.81	12.80	12.81	13.09	0.70	0.85

10x10 cm^2							
No Couch							
Gantry Angle/°	**M1/nC**	**M2/nC**	**M3/nC**	**M/nC**	**Mcor / nC**	**DW,Q**	**$N_{DW,Q}$**
0	15.09	15.08	15.08	15.08	15.41	0.83	1.00
350	15.00	15.00	15.00	15.00	15.32	0.82	0.99
340	14.74	14.74	14.74	14.74	15.06	0.81	0.98
330	14.28	14.28	14.28	14.28	14.59	0.78	0.95
320	13.49	13.50	13.50	13.50	13.79	0.74	0.89
310	12.28	12.29	12.29	12.29	12.55	0.67	0.81
300	11.48	11.48	11.48	11.48	11.73	0.63	0.76
290	12.02	12.03	12.04	12.03	12.29	0.66	0.80
280	12.31	12.31	12.31	12.31	12.57	0.68	0.82
270	12.37	12.37	12.37	12.37	12.63	0.68	0.82
Couch							
90	12.38	12.39	12.39	12.39	12.65	0.68	0.82
100	12.25	12.25	12.25	12.25	12.51	0.67	0.81
110	11.82	11.83	11.83	11.83	12.08	0.65	0.78
120	10.87	10.88	10.88	10.88	11.11	0.60	0.72
130	11.39	11.39	11.39	11.39	11.63	0.63	0.76
140	12.65	12.65	12.65	12.65	12.92	0.69	0.84
150	13.44	13.44	13.44	13.44	13.73	0.74	0.89
160	13.96	13.97	13.97	13.97	14.27	0.77	0.93
170	14.23	14.24	14.25	14.24	14.54	0.78	0.94
180	14.33	14.35	14.35	14.34	14.65	0.79	0.95

15x15 cm^2							
No Couch							
Gantry Angle/°	**M1/nC**	**M2/nC**	**M3/nC**	**M/nC**	**Mcor / nC**	**DW,Q**	**$N_{DW,Q}$**
0	15.60	15.61	15.60	15.60	15.94	0.86	1.03
350	15.52	15.53	15.53	15.53	15.86	0.85	1.03
340	15.28	15.29	15.29	15.29	15.61	0.84	1.01
330	14.86	14.85	14.85	14.85	15.17	0.82	0.98
320	14.11	14.12	14.12	14.12	14.42	0.78	0.94
310	12.92	12.95	12.94	12.94	13.21	0.71	0.86
300	12.04	12.04	12.04	12.04	12.30	0.66	0.80
290	12.67	12.67	12.67	12.67	12.94	0.70	0.84
280	13.10	13.10	13.10	13.10	13.38	0.72	0.87
270	13.11	13.11	13.11	13.11	13.39	0.72	0.87
Couch							
90	13.29	13.29	13.29	13.29	13.57	0.73	0.88
100	13.15	13.15	13.15	13.15	13.43	0.72	0.87
110	12.68	12.68	12.68	12.68	12.95	0.70	0.84
120	11.68	11.68	11.68	11.68	11.93	0.64	0.77
130	12.24	12.24	12.24	12.24	12.50	0.67	0.81
140	13.53	13.53	13.53	13.53	13.82	0.74	0.90
150	14.35	14.36	14.36	14.36	14.66	0.79	0.95
160	14.83	14.83	14.83	14.83	15.15	0.81	0.98
170	15.10	15.10	15.10	15.10	15.42	0.83	1.00
180	15.18	15.18	15.18	15.18	15.51	0.83	1.01

20x20 cm^2							
No Couch							
Gantry Angle/°	**M1/nC**	**M2/nC**	**M3/nC**	**M/nC**	**Mcor / nC**	**DW,Q**	**$N_{DW,Q}$**
0	16.19	16.20	16.20	16.20	16.54	0.89	1.07
350	16.10	16.11	16.10	16.10	16.45	0.88	1.07
340	15.88	15.89	15.88	15.88	16.22	0.87	1.05
330	15.45	15.45	15.45	15.45	15.78	0.85	1.02
320	14.73	14.73	14.73	14.73	15.05	0.81	0.98
310	13.51	13.50	13.51	13.51	13.80	0.74	0.90
300	12.61	12.61	12.61	12.61	12.88	0.69	0.84
290	13.25	13.26	13.26	13.26	13.54	0.73	0.88
280	13.73	13.73	13.73	13.73	14.02	0.75	0.91
270	13.77	13.76	13.77	13.77	14.06	0.76	0.91
Couch							
90	13.94	13.95	13.95	13.95	14.25	0.77	0.92
100	13.83	13.83	13.83	13.83	14.13	0.76	0.92
110	13.30	13.30	13.30	13.30	13.58	0.73	0.88
120	12.28	12.28	12.28	12.28	12.54	0.67	0.81
130	12.83	12.83	12.83	12.83	13.10	0.70	0.85
140	14.15	14.15	14.15	14.15	14.45	0.78	0.94
150	14.98	14.98	14.98	14.98	15.30	0.82	0.99
160	15.47	15.47	15.47	15.47	15.80	0.85	1.03
170	15.71	15.70	15.71	15.71	16.04	0.86	1.04
180	15.80	15.81	15.80	15.80	16.14	0.87	1.05

APPENDIX C 2: 15 MV Photon Energy

5x5 cm^2							
No Couch							
Gantry Angle/°	**M1/nC**	**M2/nC**	**M3/nC**	**M/nC**	**Mcor / nC**	**DW,Q**	**$N_{DW,Q}$**
0	15.11	15.11	15.11	15.11	15.43	0.83	0.90
350	15.05	15.06	15.06	15.06	15.38	0.83	0.89
340	14.85	14.85	14.85	14.85	15.17	0.82	0.88
330	14.48	14.48	14.48	14.48	14.79	0.80	0.86
320	13.84	13.84	13.84	13.84	14.14	0.76	0.82
310	12.85	12.85	12.86	12.85	13.13	0.71	0.76
300	12.02	12.03	12.03	12.03	12.28	0.66	0.71
290	12.57	12.57	12.57	12.57	12.84	0.69	0.75
280	12.90	12.90	12.90	12.90	13.18	0.71	0.77
270	12.93	12.92	12.92	12.92	13.20	0.71	0.77
Couch							
90	13.08	13.09	13.09	13.09	13.37	0.72	0.78
100	12.95	12.95	12.95	12.95	13.23	0.71	0.77
110	12.58	12.58	12.58	12.58	12.85	0.69	0.75
120	11.75	11.76	11.76	11.76	12.01	0.65	0.70
130	12.26	12.26	12.26	12.26	12.52	0.67	0.73
140	13.34	13.35	13.35	13.35	13.63	0.73	0.79
150	14.05	14.06	14.05	14.05	14.35	0.77	0.84
160	14.45	14.46	14.46	14.46	14.77	0.79	0.86
170	14.70	14.70	14.70	14.70	15.01	0.81	0.87
180	14.74	14.74	14.75	14.74	15.06	0.81	0.88

10x10 cm^2							
No Couch							
Gantry Angle/°	**M1/nC**	**M2/nC**	**M3/nC**	**M/nC**	**Mcor / nC**	**DW,Q**	**$N_{DW,Q}$**
0	16.83	16.83	16.83	16.83	17.19	0.92	1.00
350	16.77	16.76	16.77	16.77	17.13	0.92	1.00
340	16.55	16.56	16.56	16.56	16.91	0.91	0.98
330	16.17	16.16	16.17	16.17	16.51	0.89	0.96
320	15.52	15.53	15.53	15.53	15.86	0.85	0.92
310	14.48	14.48	14.48	14.48	14.79	0.80	0.86
300	13.75	13.75	13.75	13.75	14.04	0.76	0.82
290	14.24	14.24	14.24	14.24	14.54	0.78	0.85
280	14.49	14.50	14.50	14.50	14.81	0.80	0.86
270	14.53	14.53	14.53	14.53	14.84	0.80	0.86
Couch							
90	14.58	14.58	14.58	14.58	14.89	0.80	0.87
100	14.44	14.44	14.44	14.44	14.75	0.79	0.86
110	14.10	14.10	14.10	14.10	14.40	0.77	0.84
120	13.21	13.21	13.21	13.21	13.49	0.73	0.78
130	13.69	13.69	13.69	13.69	13.98	0.75	0.81
140	14.78	14.78	14.78	14.78	15.10	0.81	0.88
150	15.46	15.47	15.47	15.47	15.80	0.85	0.92
160	15.88	15.89	15.89	15.89	16.23	0.87	0.94
170	16.12	16.12	16.12	16.12	16.47	0.89	0.96
180	16.18	16.18	16.18	16.18	16.53	0.89	0.96

15x15 cm^2							
No Couch							
Gantry Angle/°	**M1/nC**	**M2/nC**	**M3/nC**	**M/nC**	**Mcor / nC**	**DW,Q**	**$N_{DW,Q}$**
0	17.24	17.24	17.24	17.24	17.61	0.95	1.02
350	17.19	17.19	17.19	17.19	17.56	0.94	1.02
340	16.99	16.99	16.99	16.99	17.35	0.93	1.01
330	16.65	16.65	16.65	16.65	17.01	0.91	0.99
320	16.04	16.04	16.04	16.04	16.38	0.88	0.95
310	15.04	15.04	15.04	15.04	15.36	0.83	0.89
300	14.23	14.23	14.23	14.23	14.53	0.78	0.85
290	14.82	14.82	14.82	14.82	15.14	0.81	0.88
280	15.19	15.20	15.20	15.20	15.52	0.83	0.90
270	15.22	15.22	15.22	15.22	15.55	0.84	0.90
Couch							
90	15.40	15.40	15.40	15.40	15.73	0.85	0.92
100	15.29	15.29	15.29	15.29	15.62	0.84	0.91
110	14.88	14.89	14.89	14.89	15.21	0.82	0.88
120	13.99	13.98	13.98	13.98	14.28	0.77	0.83
130	14.49	14.50	14.50	14.50	14.81	0.80	0.86
140	15.63	15.62	15.53	15.59	15.93	0.86	0.93
150	16.31	16.32	16.32	16.32	16.67	0.90	0.97
160	16.70	16.70	16.70	16.70	17.06	0.92	0.99
170	16.92	16.92	16.92	16.92	17.28	0.93	1.01
180	16.97	16.97	16.97	16.97	17.33	0.93	1.01

20x20 cm^2							
No Couch							
Gantry Angle/°	M1/nC	M2/nC	M3/nC	M/nC	Mcor / nC	DW,Q	$N_{DW,Q}$
0	17.75	17.73	17.74	17.74	18.12	0.97	1.05
350	17.67	17.67	17.67	17.67	18.05	0.97	1.05
340	17.50	17.50	17.50	17.50	17.87	0.96	1.04
330	17.13	17.14	17.14	17.14	17.50	0.94	1.02
320	16.57	16.58	16.58	16.58	16.93	0.91	0.98
310	15.49	15.49	15.49	15.49	15.82	0.85	0.92
300	14.72	14.72	14.71	14.72	15.03	0.81	0.87
290	15.32	15.32	15.32	15.32	15.65	0.84	0.91
280	15.73	15.75	15.75	15.74	16.08	0.86	0.94
270	15.77	15.76	15.77	15.77	16.10	0.87	0.94
Couch							
90	15.96	15.95	15.95	15.95	16.29	0.88	0.95
100	15.87	15.86	15.86	15.86	16.20	0.87	0.94
110	15.40	15.40	15.40	15.40	15.73	0.85	0.92
120	14.50	14.50	14.50	14.50	14.81	0.80	0.86
130	14.98	14.98	14.98	14.98	15.30	0.82	0.89
140	16.16	16.16	16.16	16.16	16.51	0.89	0.96
150	16.83	16.84	16.84	16.84	17.20	0.92	1.00
160	17.25	17.25	17.25	17.25	17.62	0.95	1.02
170	17.43	17.43	17.43	17.43	17.80	0.96	1.04
180	17.50	17.50	17.50	17.50	17.87	0.96	1.04

APPENDIX D: Attenuation Correction Factors for the various field sizes and gantry angles

		6 MV				15 MV			
Gantry Angle/°	**Predicted CF**	**5x5cm²**	**10x10cm²**	**15x15cm²**	**20x20cm²**	**5x5cm²**	**10x10cm²**	**15x15cm²**	**20x20cm²**
180	1.0534	1.0400	1.0516	1.0279	1.0249	1.0249	1.0402	1.0160	1.0137
170	1.0542	1.0400	1.0534	1.0283	1.0253	1.0243	1.0401	1.0160	1.0138
160	1.0569	1.0440	1.0554	1.0308	1.0267	1.0272	1.0422	1.0170	1.0145
150	1.0619	1.0510	1.0625	1.0346	1.0314	1.0304	1.0453	1.0200	1.0178
140	1.0702	1.0580	1.0669	1.0434	1.0410	1.0370	1.0505	1.0290	1.0258
130	1.0843	1.0720	1.0787	1.0569	1.0527	1.0484	1.0577	1.0380	1.0340
120	1.1096	1.0380	1.0555	1.0308	1.0269	1.0230	1.0409	1.0180	1.0149

APPENDIX E: Clinical Validation Measurements

Gantry angle/	TPS Cor dMax	SSD1	SSD2	Actual Dmax	Linac Dmax	Diff	%Diff
6 MV							
180	0.44	93.2	88.20	0.49	0.52	0.0552	6%
170	0.44	92.5	87.42	0.49	0.52	0.0526	5%
160	0.45	90.9	85.58	0.51	0.53	0.0421	4%
150	0.47	89.7	83.93	0.54	0.57	0.0582	6%
140	0.49	88.4	81.87	0.57	0.59	0.0317	3%
130	0.52	86.9	79.12	0.63	0.65	0.0349	3%
120	0.52	85.3	75.30	0.67	0.71	0.0602	6%
15 MV							
180	0.39	93.2	88.20	0.44	0.46	0.0533	5%
170	0.39	92.5	87.42	0.44	0.47	0.0710	7%
160	0.39	90.9	85.58	0.44	0.47	0.0638	6%
150	0.41	89.7	83.93	0.47	0.50	0.0634	6%
140	0.43	88.4	81.87	0.5	0.52	0.0359	4%
130	0.45	86.9	79.12	0.54	0.57	0.0476	5%
120	0.45	85.3	75.30	0.58	0.61	0.0533	5%